International Journal of Mechanical, Industrial and Aerospace Sciences
ISSN: 2517-9950
Vol:2, No:3, 2008

Modeling and FOS Feedback Based Control of SISO Intelligent Structures with Embedded Shear Sensors and Actuators

T.C. Manjunath[1], *Student Member IEEE* , B. Bandyopadhyay[2], *member IEEE*

Abstract**—**Active vibration control is an important problem in structures. The objective of active vibration control is to reduce the vibrations of a system by automatic modification of the system's structural response. In this paper, the modeling and design of a fast output sampling feedback controller for a smart flexible beam system embedded with shear sensors and actuators for SISO system using Timoshenko beam theory is proposed. FEM theory, Timoshenko beam theory and the state space techniques are used to model the aluminum cantilever beam. For the SISO case, the beam is divided into 5 finite elements and the control actuator is placed at finite element position 1, whereas the sensor is varied from position 2 to 5, i.e., from the nearby fixed end to the free end. Controllers are designed using FOS method and the performance of the designed FOS controller is evaluated for vibration control for 4 SISO models of the same plant. The effect of placing the sensor at different locations on the beam is observed and the performance of the controller is evaluated for vibration control. Some of the limitations of the Euler-Bernoulli theory such as the neglection of shear and axial displacement are being considered here, thus giving rise to an accurate beam model. Embedded shear sensors and actuators have been considered in this paper instead of the surface mounted sensors and actuators for vibration suppression because of lot of advantages. In controlling the vibration modes, the first three dominant modes of vibration of the system are considered.

Keywords**—**Smart structure, Timoshenko beam theory, Fast output sampling feedback control, Finite Element Method, State space model, SISO, Vibration control, LMI.

I. INTRODUCTION

IN recent years, smart materials for vibration control of structures have attracted much attention in the field of vibration control and considerable effort has been focused on the development of smart materials and structures. These structures have the ability to adapt to their environments through shape or material property modifications using piezoelectric sensors and actuators. Smart materials such as Piezoelectrics, MR Fluids, Piezoceramics, ER Fluids, Shape Memory Alloys, PVDF, make the structure **intelligent**, smart and self-adapting. The application of this technology is numerous and they include vibration control in aircrafts, active noise and shape control, acoustic control, control of antennas, control of space structures and in the control of flexible manipulators. Beams are subjected to vibrations when external forces act upon them as shown in Fig. 1 and they have to be controlled. The smart materials embedded inside the structure generate another response, which in turn interacts with the original response of the system, thereby reducing the vibrations using destructive interference.

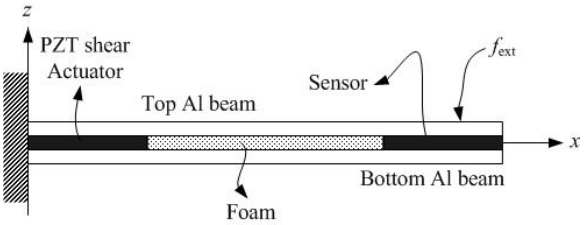

Fig. 1 A flexible sandwiched Timoshenko beam with embedded shear sensor and actuator with disturbing force applied at free end

A large number of applications of piezoelectric actuators and sensors have been proposed and demonstrated for vibration suppression in recent years. The early studies are mostly focused on surface glued piezoceramics which has some disadvantages such as difficulties to protect the ceramics and the connection wires, bad coupling with only on surface glued on the base materials, low-signal-to-noise ratio, e.t.c.,. These problems can be solved with the embedded piezoceramics. This paper deals with the active vibration control using embedded piezoelectrics as both actuators and sensors. The greatest advantage provided by the adaptive sandwich beam with embedded shear sensors / actuators is, the sensors and actuators being protected from the external environment. Since piezo-ceramics are very brittle, high stresses are detrimental to the structural integrity of the actuator.

Long-term usage of the actuator can be ensured if stresses in the actuator are low. For the sandwich structure, the actuator sustains the lowest bending stress level within the

[1]Mr. Tadaga Channaveerappa Manjunath is a Research Scholar (student member IEEE, IOP, SPIE and a life member of ISOI, ISSS, SSI, ISTE) in the Interdisciplinary Programme in Systems and Control Engineering, Indian Institute of Technology Bombay, Powai, Mumbai-400076, Maharashtra, India. (Corresponding author phone : +91 22 25780263 / 25767884 ; Fax: +91 22 25720057 ; E-mail: tcmanju@sc.iitb.ac.in, tcmanjunath@gmail.com, URL : http://www.sc.iitb.ac.in/~tcmanju).

[2]Dr. Bijnan Bandyopadhyay is with the Interdisciplinary Programme in Systems and Control Engineering, Indian Institute of Technology Bombay, IIT Bombay, Mumbai-76, Maharashtra, India and is currently in the Professor cadre. (Phone : +91 22 25767889 / Fax: +91 22 25720057 ; Email : bijnan@ee.iitb.ac.in, URL : http://www.sc.iitb.ac.in/~bijnan).

structure because the piezoelectric core is located near the neutral plane of the beam. For the surface mounted actuation beam, the piezoelectric actuators bear the largest bending stress level in the structure since the actuators are located at the farthest locations from the neutral plane and the fault occurs at the piezo-patches.

Numerous identification and control techniques have been proposed for active vibration suppression of smart flexible structures by various researchers. Some of the various methods used for active vibration control in systems are the Periodic Output Feedback (POF) control [23], sliding mode control (continuous, discrete, higher order), H_2 and H_∞ control, Fast Output Sampling (FOS) feedback control [20] [21] [25], independent modal space control method, modified independent modal space control method, positive position feedback control and the PID control.

In this paper, a flexible aluminum cantilever beam of suitable dimensions is considered. The beam is divided into 5 finite elements and shear PZT's are embedded into the master structure. The actuator is sandwiched in between the 2 aluminum beam layers at finite element position 1 and the sensor is moved from 2nd position to the 5th position, thus giving rise to 4 SISO models of the same plant. These models are obtained using the theory of piezoelectric bonding, the Timoshenko beam theory, FEM technique and the state space techniques by considering the first 3 dominant vibratory modes ω_1, ω_2 and ω_3 [26], [27], [33]. An external force input f_{ext} is applied at the free end of the beam for all the 4 models of the plant. There are two inputs to the plant. One is the external force input f_{ext}, which is taken as a load matrix of 1 unit in the simulation. The other input is the control input u to the actuator from the controller.

The paper is presented in the following sequence. A brief review of related literature about the types of beam models and embedded shear actuation is given in section 2. Section 3 gives a brief introduction to the modeling technique (finite element model, sensor and actuator model, state space model) of the smart flexible cantilever beam using Timoshenko beam theory. A brief review of the controlling technique, viz., the fast output sampling feedback control technique and the design of the proposed controller to control the first three dominant modes of vibration of the system for different embedded sensor locations along the length of the beam for the various SISO models of the same plant is discussed in Section 4. The control simulation results and discussions are presented in Section 5. Section 6 concludes the paper with conclusions.

II. A Brief Review of Beam Models

The study of physical systems such as beams frequently results in partial differential equations, which either cannot be solved analytically, or lack an exact analytic solution due to the complexity of the boundary conditions. For a realistic and detailed study, a numerical method must be used to solve the problem. The finite element method [35] is often found the most adequate. Over the years, with the development of modern computers, the finite element method [35] has become one of the most important analysis tools in engineering. Basically, the finite element method consists of a piecewise application of classical variational methods to smaller and simpler sub domains called finite elements connected to each other in a finite number of points called nodes. A precise mathematical model is required for the controller design for vibration control to predict the structure's response. Two beam models in common use in the structural mechanics are the Euler-Bernoulli beam model and the Timoshenko beam model, which are considered here below.

A. Euler-Bernoulli Model

In this model [2] [3] [5] [10], bending effects on stresses, moments and deformations are considered. The effect of shear, axial displacement is neglected as a result of which accurate model of the system is not available for sophisticated control. The assumption that we make while developing this model is that the cross sections of the beams remain plane and normal to the deformed longitudinal axis before and after bending as shown in Fig. 2. The total rotation θ is due to bending stress alone neglecting transverse shear stress. This rotation occurs about a neutral axis that passes through the centroid of the cross section. Euler-Bernoulli beam theory gives inaccurate results for very higher modes of vibration because the shear forces and the axial displacements are neglected; therefore, a controller based on *Euler Bernoulli Beam Theory* will not perform satisfactorily in controlling the higher modes of vibration of a structure. This assumption is valid if length to thickness ratio is large and for small deflection of beam. However, if length to thickness ratio is small, plane section before bending will not remain normal to the neutral axis after bending.

Many researchers have extensively worked on the active vibration control of structures using the Euler-Bernoulli method. To mention a few, Crawley *et.al.* [2] have presented the analytical and experimental development of piezoelectric actuators as elements of **intelligent** structures. The difficulty in the smart structure FE model faced by the control system engineers and the advantage offered in structural mechanics point of view and the method to get a reduced order model can be seen in [11]. A number of experiments were performed by Fanson *et.al.* [34] with piezoelements using positive feedback. Yang and Lee [1] developed an analytical model for structural control optimization in which both the non-collocated sensor / actuator placement and feedback control gain were considered as independent variables. Continuous time and discrete time algorithms were proposed to control a thin piezoelectric structure in [4].

The concept of smart structures was presented in the survey paper by Culshaw [22] and Rao [6]. Smart structures and its numerous applications was presented by Baily and Hubbard [5]. Hwang and Park [10] presented a new FE modeling technique for flexible beams. An effective vibration control

scheme using periodic output feedback technique was presented by Manjunath and Bandyopadhyay in [23]. The effect of failure of one of the actuators in a multivariable smart system and its control using the periodic output feedback control law was discussed in [24]. In [25], Manjunath and Bandyopadhyay presented the best model for the best location of the placement of sensor / actuator out of the different models for three types of systems.

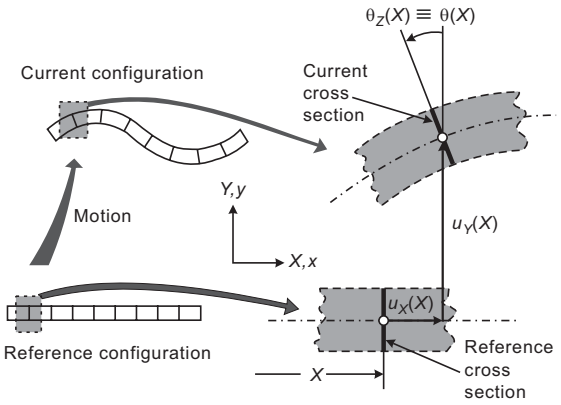

Fig. 2 Euler-Bernoulli beam model

B. Timoshenko model

This model [8] [9] [12] - [15], [37] takes into account the axial displacement and the shear into consideration while developing the model for the structure and thus corrects the drawbacks and the assumptions made in Euler-Bernoulli model Theory. The cross sections remain plane and rotate about the same neutral axis as the Euler-Bernoulli model, but do not remain normal to the deformed longitudinal axis as shown in Fig. 3. The deviation from normality is produced by a transverse shear that is assumed to be constant over the cross section. The total slope of the beam consists of two parts, one due to bending θ, and the other due to shear β. Because of the above-mentioned reasons, the Timoshenko Beam model is far more superior to the Euler-Bernoulli model in precisely predicting the beam response. Timoshenko Beam theory is used in the present work to generate the FE model of a flexible cantilever beam with embedded shear piezoelectric patches in between two flexible aluminum beams. Further, the fast output sampling feedback control design and its application to control the structural vibration modes of a smart cantilever beam are considered.

A survey of some advances in the embedded technology of smart structures is done here. Aldraihem *et al.* [13] have developed a laminated beam model using two theories; namely, Euler-Bernoulli beam theory and Timoshenko Beam theory. Abramovich [14] has presented analytical formulation and closed form solutions of composite beams with piezoelectric actuators, which was based on Timoshenko beam theory. Using a higher-order shear deformation theory, Chandrashekhara and Varadarajan [12] presented a finite element model of a composite beam to produce a desired deflection in beams with clamped-free (C-F), clamped-clamped (C-C) and simply supported ends. Shear embedded piezoelectrics are used nowadays to suppress the vibrations. Sun and Zhang [9], [15] suggested the idea of exploiting the shear mode to create transverse deflection in sandwich structures. Here, he proved that embedded shear actuators offer many advantages over surface mounted extension actuators.

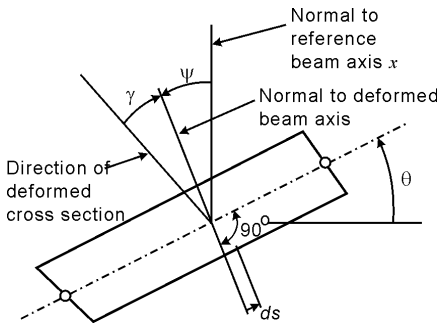

Fig. 3 Timoshenko beam model

Aldraihem and Khdeir [18] proposed analytical models and exact solutions for beams with shear and extension piezoelectric actuators and the models were based on Timoshenko beam theory and higher-order beam theory (HOBT). Exact solutions were obtained by using the state-space approach. In a more recent work, Zhang and Sun [15] formulated an analytical model of a sandwich beam with shear piezoelectric actuator that occupies the entire core. The model derivation was simplified by assuming that the face layers follow Euler-Bernoulli beam theory, whereas the core layer obeys Timoshenko beam theory. Furthermore, a closed form solution of the static deflection was presented for a cantilever beam. Abramovich [14] studied the effects of actuator location and number of patches on the actuator's performance for various configurations of the piezo patches and boundary conditions under mechanical and / or electric loads.

A finite element approach was used by Benjeddou *et. al.* [17] to model a sandwich beam with shear and extension piezoelectric elements. The finite element model employed the displacement field of Zhang and Sun [9] [15]. It was shown that the finite element results agree quite well with the analytical results. Raja *et. al.* [16] extended the finite element model of Benjeddou's research team to include a vibration control scheme. Deflection analysis of beams with extension and shear piezoelectric patches was reported by Ahmed and Osama [28]. An improved two-node Timoshenko beam model was presented by Friedman and Kosmataka [26] which is used in our work. Azulay *et al.* [27] have presented analytical formulation and closed form solutions of composite beams with piezoelectric actuators.

III. Mathematical Modeling of Smart Sandwiched Beam with Embedded Shear Sensors and Actuators

Many researchers have well established a mathematical finite element E-B model. These models do not consider the shear effects, axial effects, etc.,.. Modeling of embedded smart

structures using shear deformable (Timoshenko) theory is limited. In our work, the effect of shear and axial displacement has been considered in modeling. In this section, a shear deformable (Timoshenko) Finite Element Model is developed for a laminated beam and its application in active vibration control is investigated [26], [27], [33]. Accurate model of the system is obtained when the shear effects and the axial displacement of the beam is considered in modeling of the smart structure.

A. Finite Element Modeling [F E M] of the Sandwiched Beam Element

A sandwiched beam (piezo-laminated composite beam) is shown in Fig. 4 and consists of 3 layers, viz., the piezo-*patch* with the rigid foam is sandwiched in between two aluminum beam layers. For shear actuation, rigid foam is introduced as a core along with PZT to obtain an equivalent sandwiched model. The ***assumption*** made is that the middle layer is perfectly glued to the carrying structure and the thickness of the adhesive is neglected (thus, neglecting the effect of shear-lag, no slippage or delamination between the core layers during vibrations) as a result of which strong coupling exists between the master structure and the piezo-patches.

The perfect bonding or the adhesive between the beam and the sensor / actuator and the bottom and top surfaces of the upper and lower aluminum beam have been assumed to add no mass or stiffness to the sensor / actuator. For the parts without piezoelectrics, the extra space at places where no piezoelectrics is present is being packed up fully with a non-structural material, like rigid foam and it is assumed that its material properties are assumed to be zero and the bending angle of aluminum is assumed to be almost equal to that of the rigid foam (as there is strong coupling between the rigid foam and the structure). The beam is stacked properly and then used as a composite structure for AVC. Thus, sandwich structures consisting of sheets and a relatively light-weight core such as honeycomb or rigid foam are highly efficient in producing bending and shear [9], [15].

In the modeling of the structure, only the properties of the piezopatches and the beam are considered. The poling direction of the piezoelectric patch is along the x (axial) direction. The displacement field is based on a first order shear deformation theory. The element has constant moment of inertia, modulus of elasticity, mass density and length. The cable capacitance between sensor and signal-conditioning device has been considered negligible and the temperature effects have been neglected. The signal conditioning device gain (G_c) is assumed as 100. The longitudinal axis of the sandwiched beam element lies along the X-axis and the beam is subjected to vibrations in the X - Z plane. The beam element is assumed to have three structural DOF, viz., (w, θ) at each nodal point, w being the transverse displacement and an axial displacement (u) of the nodal point.

A bending moment and a transverse shear force acts at each nodal point. dw/dx is the slope of the beam (composed of 2 parts, $\theta(x)$, the bending slope and the additional shear deformation $\gamma(x)$). ψ is the rotational angle of the core material. An additional DOF, called as the electrical DOF (sensor voltage) comes into picture. Since the voltage is constant over the electrode, the number of electrical DOF is one for each element.

TABLE I
PROPERTIES OF THE FLEXIBLE AL CANTILEVER BEAM ELEMENT

Parameter (with units)	Symbol	Numerical values
Length (cm)	l_b	30
Width (cm)	c	2
Thickness of the top layer and bottom Al beam layers (mm)	t_b	1
Young's modulus (GPa)	E_b	193.06
Density (kg/m^3)	ρ_b	8030
Structural constants	$\alpha,\ \beta$	0.001. 0.0001

TABLE II
PROPERTIES OF THE PIEZO - SENSOR / ACTUATOR ELEMENT

Parameter (with units)	Symbol	Numerical values
Length (cm)	l_p	6
Width (cm)	c	2
Thickness (mm)	t_a, t_s	1
Young's modulus (GPa)	E_p	68
Density (kg/m^3)	ρ_p	7700
Piezo strain constant (m / V)	d_{31}	125×10^{-12}

The equations of motion of a general piezo-laminated composite beam is obtained as follows [26], [27], [33]. The displacements of the beam $u(x)$ and $w(x)$ can be written as

$$u(x,z) = u_0(x) + z\theta(x,t), \quad (1)$$

$$w(x,z) = w_0(x), \quad (2)$$

where $u_0(x)$ and $w_0(x)$ are the axial and lateral displacements of the point at the mid-plane assuming that there is incompressibility in the z direction and $\theta(x)$ is the bending rotation of the normal to the mid-plane, i.e., rotation of the beam about the y axis. The total strain vector is the sum of the mechanical strain vector and the actuator induced strain vector. The strain components of the beam are given as

$$\varepsilon_x = \frac{\partial u_0}{\partial x} + z\frac{\partial \theta}{\partial x}, \quad (3)$$

$$\varepsilon_z = 0, \quad (4)$$

$$\gamma_{xz} = \frac{\partial u}{\partial x} + \frac{\partial w_0}{\partial x} = \theta + \frac{\partial w_0}{\partial x}. \quad (5)$$

where $\varepsilon_x, \varepsilon_z$ are the mechanical normal and transverse shear strain, γ_{xz} being the shear strain induced in the piezoelectric layer. The beam constitutive equation can be written as

$$\begin{bmatrix} N_x \\ M_x \\ Q_{xz} \end{bmatrix} = \begin{bmatrix} A_{11} & B_{11} & 0 \\ B_{11} & D_{11} & 0 \\ 0 & 0 & A_{55} \end{bmatrix} \begin{bmatrix} \dfrac{\partial u_0}{\partial x} \\ \dfrac{\partial \theta}{\partial x} \\ \theta + \dfrac{\partial w_0}{\partial x} \end{bmatrix} - \begin{bmatrix} E_{11} \\ F_{11} \\ G_{55} \end{bmatrix}, \quad (6)$$

$$N_x = \int_{-h/2}^{h/2} c\,\sigma_x\,dz, \quad (7)$$

$$M_x = \int_{-h/2}^{h/2} c\,\sigma_x\,z\,dz, \quad (8)$$

$$Q_{xz} = \int_{-h/2}^{h/2} c\,\tau_{xz}\,dz. \quad (9)$$

Here, $\sigma_x = \overline{Q}_{11}\,\varepsilon_x$ and $\tau_{xz} = \overline{Q}_{55}\,\gamma_{xz}$ are the normal and shear stresses respectively and c is the width of the beam. z is the depth of the material point measured from the beam reference plane along the vertical axis. h is the height of the beam + piezo - patch, i.e., the thickness of the total structure which includes t_b, t_a, t_s (thickness of beam, thickness of actuator / sensor). N_x, M_x, Q_{xz} are the internal forces acting on the cross section of the beam. A_{11}, B_{11}, D_{11} and A_{55} are the extensional, bending-extensional, bending and transverse shear stiffness coefficients defined according to the lamination theory as

$$A_{11} = c\sum_{k=1}^{N}\left(\overline{Q}_{11}\right)_k\left(z_k - z_{k-1}\right), \quad (10)$$

$$B_{11} = \frac{c}{2}\sum_{k=1}^{n}\left(\overline{Q}_{11}\right)_k\left(z_k^2 - z_{k-1}^2\right), \quad (11)$$

$$D_{11} = \frac{c}{3}\sum_{k=1}^{N}\left(\overline{Q}_{11}\right)_k\left(z_k^3 - z_{k-1}^3\right), \quad (12)$$

$$A_{55} = c\,K\sum_{k=1}^{N}\left(\overline{Q}_{55}\right)_k\left(z_k - z_{k-1}\right). \quad (13)$$

Here, in Eqns. (10) to (13), z_k is the distance of the k^{th} layer from the x-axis, N is the number of layers, K is the shear correction factor usually taken equal to $\frac{5}{6}$ and $\overline{Q}_{11}$, $\overline{Q}_{55}$ are calculated according to the equations using the material properties of the piezoelectric material as given by

$$\overline{Q}_{11} = Q_{11}\cos^4\lambda + Q_{22}\sin^4\lambda + 2\left(Q_{12} + 2Q_{66}\right)\sin^2\lambda\,\cos^2\lambda, \quad (14)$$

$$\overline{Q}_{55} = G_{13}\cos^2\lambda + G_{23}\sin^2\lambda. \quad (15)$$

The angle λ is the angle between the fiber direction and the longitudinal axis of the beam. The material constants Q_{11}, Q_{22}, Q_{12}, Q_{66}, Q_{13} and Q_{23} for foam, aluminum and piezoelectric material was taken from the data handbook. These constants are used to calculate the values of A_{11}, B_{11}, D_{11} and A_{55} using Eqns. (10) to (15). E_{11}, F_{11} and G_{55} in Eqn. (6) are the actuator induced axial force, bending moment and the shear force respectively, defined as

$$E_{11} = c\sum_{k=1}^{N_a}\left(\overline{Q}_{11}\right)_k^a V^k(x,t)\,d_{31}^k, \quad (16)$$

$$F_{11} = \frac{c}{2}\sum_{k=1}^{N_a}\left(\overline{Q}_{11}\right)_k^a V^k(x,t)\,d_{31}^k\left(z_{k+}^a - z_{k-}^a\right), \quad (17)$$

$$G_{55} = c\,K\sum_{k=1}^{N_a}\left(\overline{Q}_{55}\right)_k^a V^k(x,t)\left(d_{15}^k\right). \quad (18)$$

Since the piezoelectric layer is poled in the axial direction, $E_{11} = F_{11} = 0$. $V_k(x,t)$ is the applied voltage to the k^{th} actuator having a thickness of $\left(z_{k+}^a - z_{k-}^a\right)$ and d_{31}^k, d_{15}^k are the piezoelectric constants. $\left(\overline{Q}_{55}\right)_k^a$ and $\left(\overline{Q}_{11}\right)_k^a$ are the coefficients of the actuators calculated using the equations (14) and (15). N_a is the number of actuators, where 'a' stands for 'w.r.t. actuator'. Using the Hamilton's principle (total strain energy is equal to the sum of the change in the kinetic energy + the work done due to the external forces), we get

$$\delta\Pi = \int_{t_1}^{t_2}\int_{0}^{L}\left(\delta T - \delta U + \delta W\right)dx\,dt, \quad (19)$$

where

T is kinetic energy,
U is strain energy,
W is the external work done,
L is the length of the beam element and
t is the time.

The strain energy U of the beam element is given by

$$\delta U = N_x\left(\frac{\partial\,\delta u}{\partial x}\right) + M_x\left(\frac{\partial\,\delta\theta}{\partial x}\right) + Q_{xz}\left(\theta + \frac{\partial\,\delta w}{\partial x}\right). \quad (20)$$

The kinetic energy T of the beam element is given by

$$\delta T = \left(I_1\dot{u} + I_2\dot{\theta}\right)\partial\dot{u} + I_1\dot{w}\partial\dot{w} + \left(I_2\dot{u} + I_3\dot{\theta}\right)\partial\dot{\theta}. \quad (21)$$

Here, in Eqn. (21), I_1, I_2 and I_3 are the mass inertias

defined as

$$I_1 = c \int_{-h/2}^{h/2} \rho \, dz, \tag{22}$$

$$I_2 = c \int_{-h/2}^{h/2} z \, \rho \, dz, \tag{23}$$

$$I_3 = c \int_{-h/2}^{h/2} z^2 \rho \, dz, \tag{24}$$

where ρ is the mass density of each layer, c being the width of the beam and h is the height of the beam + piezo - patch, i.e., the thickness of the total structure.

The external work done (i.e., force×displacement) is given as

$$\delta W = q_0 \, \delta w, \tag{25}$$

where q_0 is the transverse distributed loading. Substituting the values of strain energy, kinetic energy and external work done from Eqns. (20), (21) and (25) into Eqn. (19), we get the governing equation of motion of a general shaped non-symmetric piezo-laminated beam with shear deformation and rotary inertia as

$$\frac{\partial}{\partial x}\left(A_{11}\frac{\partial u}{\partial x} + B_{11}\frac{\partial \theta}{\partial x} + E_{11} \right) = \frac{\partial}{\partial t}\left[(I_1 \dot{u}) + (I_2 \dot{\theta}) \right], \tag{26}$$

$$\frac{\partial}{\partial x}\left(A_{55}\left(\theta + \frac{\partial w}{\partial x} \right) + G_{55} \right) = \frac{\partial}{\partial t}\left[(I_1 \dot{w}) + q_0 \right], \tag{27}$$

$$\frac{\partial}{\partial x}\left(B_{11}\frac{\partial u}{\partial x} + D_{11}\frac{\partial \theta}{\partial x} + F_{11} \right) - A_{55}\left(\theta + \frac{\partial w}{\partial x} \right) - G_{55} = \frac{\partial}{\partial t}\left[(I_3 \dot{\theta}) + (I_2 \dot{u}) \right], \tag{28}$$

which becomes

$$\frac{\partial}{\partial x}\left(A_{11}\frac{\partial u}{\partial x} + B_{11}\frac{\partial \theta}{\partial x} \right) = 0, \tag{29}$$

$$\frac{\partial}{\partial x}\left(A_{55}\left(\theta + \frac{\partial w}{\partial x} \right) \right) = 0, \tag{30}$$

$$\frac{\partial}{\partial x}\left(B_{11}\frac{\partial u}{\partial x} + D_{11}\frac{\partial \theta}{\partial x} \right) - A_{55}\left(\theta + \frac{\partial w}{\partial x} \right) - G_{55} = 0 \tag{31}$$

for a static case and with constant properties of the beam. To facilitate the solution process for the coupled equations in equations (29)-(31), the beam stiffness A_{55} and D_{11} are assumed to be uniform and constant throughout the beam length [26], [27], [33]. Note that the influence of shear-induced strains appears in the above-coupled equations of motion for constant properties along the beam. Let

$$w = a_1 + a_2 \, x + a_3 \, x^2 + a_4 \, x^3, \tag{32}$$

$$\theta = b_1 + b_2 \, x + b_3 \, x^2, \tag{33}$$

$$u = c_1 + c_2 \, x + c_3 \, x^2 \tag{34}$$

be the solutions of the Eqns. (29) to (31) where a_i, b_j and c_j's are the unknown coefficients $(i=1,.....,4)$ and $(j=1,.....,3)$ subject to the boundary conditions

$$\begin{aligned} \text{at} \quad x = 0 \quad & w = w_1 \quad \theta = \theta_1 \quad u = u_1, \\ x = L \quad & w = w_2 \quad \theta = \theta_2 \quad u = u_2, \end{aligned} \tag{35}$$

where x is the local axial coordinate of the element. After applying boundary conditions from Eqn. (35) into Eqns. (32)-(34), the unknown coefficients a_i, b_j and c_j's can be resolved. Since the axial displacement of a point not on the centerline is a linear function of θ as well as u, the degree of the polynomial used for θ must be the same as that used for u. In addition, the shear strain is a linear function of both θ and dw/dz. Consequently, the degree of the polynomial used for w must be one order higher than those used for u and θ in order to ensure compatibility. Therefore, the cubic polynomial used for the displacement w requires that quadratic functions be used for both axial displacement u and cross section rotation θ in order to be consistent. Then, substituting the found out unknown coefficients into equations (32)-(34) and writing them in matrix form, we get the expression for the axial displacement, transverse displacement and the bending rotation as

$$[u] = [N_u] \begin{Bmatrix} u_1 \\ w_1 \\ \theta_1 \\ u_2 \\ w_2 \\ \theta_2 \end{Bmatrix}, \tag{36}$$

$$[w] = [N_w] \begin{Bmatrix} w_1 \\ \theta_1 \\ w_2 \\ \theta_2 \end{Bmatrix}, \tag{37}$$

and

$$[\theta] = [N_\theta] \begin{Bmatrix} w_1 \\ \theta_1 \\ w_2 \\ \theta_2 \end{Bmatrix}, \tag{38}$$

where N_u, N_w N_θ are the mode shape functions due to the axial displacement, transverse displacement and due to the rotation or the slope, which are defined as

$$[N_u] = [N_1 \quad N_2 \quad N_3 \quad N_4 \quad N_5 \quad N_6], \tag{39}$$

$$[N_w] = [N_7 \quad N_8 \quad N_9 \quad N_{10}], \tag{40}$$

$$[N_\theta] = [N_{11} \quad N_{12} \quad N_{13} \quad N_{14}] \tag{41}$$

with the elements of the shape function given by

$$N_1 = 1 - \frac{x}{l}, \tag{42}$$

$$N_2 = \frac{6\gamma}{(12\eta - l^2)}\, x - \frac{6\gamma}{l(12\eta - l^2)}\, x^2, \tag{43}$$

$$N_3 = -\frac{6\gamma}{(12\eta - l^2)}\, x + \frac{6\gamma}{l(12\eta - l^2)}\, x^2, \tag{44}$$

$$N_4 = \frac{x}{l}, \tag{45}$$

$$N_5 = -\frac{3\gamma l}{(12\eta - l^2)}\, x + \frac{3\gamma}{(12\eta - l^2)}\, x^2, \tag{46}$$

$$N_6 = -\frac{3\gamma l}{(12\eta - l^2)}\, x + \frac{3\gamma}{(12\eta - l^2)}\, x^2, \tag{47}$$

$$N_7 = 1 - \frac{12\eta}{l(12\eta - l^2)}\, x + \frac{3}{(12\eta - l^2)}\, x^2 - \frac{2}{l(12\eta - l^2)}\, x^3, \tag{48}$$

$$N_8 = \left(\frac{6\eta}{(12\eta - l^2)} - 1\right) x - \frac{x^2}{2l} - \frac{3}{2}\frac{l}{(12\eta - l^2)}\, x^2 + \frac{1}{(12\eta - l^2)}\, x^3, \tag{49}$$

$$N_9 = \frac{12\eta}{l(12\eta - l^2)}\, x - \frac{3}{(12\eta - l^2)}\, x^2 + \frac{2}{l(12\eta - l^2)}\, x^3, \tag{50}$$

$$N_{10} = \frac{6\eta}{(12\eta - l^2)} x - \frac{x^2}{2l} - \frac{3}{2}\frac{l}{(12\eta - l^2)}\, x^2 + \frac{1}{(12\eta - l^2)}\, x^3, \tag{51}$$

$$N_{11} = -\frac{6}{(12\eta - l^2)} x + \frac{6}{l(12\eta - l^2)}\, x^2, \tag{52}$$

$$N_{12} = 1 - \frac{x}{l} + \frac{3l}{(12\eta - l^2)} x - \frac{3}{(12\eta - l^2)}\, x^2, \tag{53}$$

$$N_{13} = -\frac{6}{(12\eta - l^2)} x - \frac{6}{l(12\eta - l^2)}\, x^2, \tag{54}$$

$$N_{14} = \frac{x}{l} + \frac{3\,l}{(12\eta - l^2)}\, x - \frac{3}{(12\eta - l^2)}\, x^2, \tag{55}$$

and

$$\gamma = \frac{B_{11}}{A_{11}}, \tag{56}$$

$$\eta = \frac{D_{11}}{A_{55}}\left(\frac{\gamma B_{11}}{D_{11}} - 1\right) \tag{57}$$

as the constants, which are, being expressed in terms of bending and shear stiffness coefficients. Writing the 3 shape functions N_u, N_w N_θ in matrix form, we get the relation between the vector of inertial forces N and the vector of nodal displacements $\mathbf{q}$ (displacement field) as $\{\mathrm{N}\} = [S]\{\mathbf{q}\}$ which is given by

$$[N] = \begin{bmatrix} N_1 & N_2 & N_3 & N_4 & N_5 & N_6 \\ 0 & N_7 & N_8 & 0 & N_9 & N_{10} \\ 0 & N_{11} & N_{12} & 0 & N_{13} & N_{14} \end{bmatrix} \begin{bmatrix} u_1 \\ w_1 \\ \theta_1 \\ u_2 \\ w_2 \\ \theta_2 \end{bmatrix}. \tag{58}$$

The mass matrix of the particular regular beam element is given by

$$[M] = \int_0^l [N]^T [I][N]\, dx, \tag{59}$$

where

$$[I] = \begin{bmatrix} I_1 & 0 & I_2 \\ 0 & I_1 & 0 \\ I_2 & 0 & I_3 \end{bmatrix} \tag{60}$$

is the inertia matrix and I_1, I_2 and I_3 are given by Eqns. (22) to (24) respectively. The element mass matrix is given by [29]

$$[M] = \begin{bmatrix} M_{11} & M_{12} & M_{13} & M_{14} & M_{15} & M_{16} \\ M_{21} & M_{22} & M_{23} & M_{24} & M_{25} & M_{26} \\ M_{31} & M_{32} & M_{33} & M_{34} & M_{35} & M_{36} \\ M_{41} & M_{42} & M_{43} & M_{44} & M_{45} & M_{46} \\ M_{51} & M_{52} & M_{53} & M_{54} & M_{55} & M_{56} \\ M_{61} & M_{62} & M_{63} & M_{64} & M_{65} & M_{66} \end{bmatrix}. \tag{61}$$

Here, $[M]$ is a symmetric matrix called as the local matrix, i.e., the mass matrix of the small finite element [30]-[32]. The values of the mass matrix coefficients are given in the appendix. The stiffness matrix of the particular regular beam element [29] is given by

$$[K] = \int_0^l [B]^T [D][B]\, A\, dx, \tag{62}$$

where A is the area of cross section and

$$[B] = \frac{d[N]}{dx}, \tag{63}$$

$$[D]=\begin{bmatrix} A_{11} & B_{11} & 0 \\ B_{11} & D_{11} & 0 \\ 0 & 0 & A_{55} \end{bmatrix}, \quad (64)$$

$$[K]=\begin{bmatrix} K_{11} & K_{12} & K_{13} & K_{14} & K_{15} & K_{16} \\ K_{21} & K_{22} & K_{23} & K_{24} & K_{25} & K_{26} \\ K_{31} & K_{32} & K_{33} & K_{34} & K_{35} & K_{36} \\ K_{41} & K_{42} & K_{43} & K_{44} & K_{45} & K_{46} \\ K_{51} & K_{52} & K_{53} & K_{54} & K_{55} & K_{56} \\ K_{61} & K_{62} & K_{63} & K_{64} & K_{65} & K_{66} \end{bmatrix}. \quad (65)$$

Here, $[K]$ is a symmetric matrix called as the local matrix [30]-[32]. The values of the matrix coefficients are given in the appendix. The mass and stiffness matrices of the regular beam element are obtained using foam as the core between two facing aluminum layers. The mass and stiffness matrices of the piezoelectric beam element are obtained by using a shear piezoelectric patch between the two facing aluminum layers.

B. Sensor and Actuator Equations

In this section, modeling of the sensor and actuator equation is presented.

1) Sensor Equation

When a force acts upon a piezoelectric material, electric field is produced [6] [22]. This effect, which is called as the direct piezoelectric effect, is used to calculate the output charge produced by the strain in the structure. The external field produced by the sensor is directly proportional to the strain rate. The charge $q(t)$ accumulated on the piezoelectric electrodes using the gauss law is given by

$$\mathbf{q}(t) = \iint_A D_3 \, dA, \quad (66)$$

where D_3 is the electric displacement in the thickness direction and A is the area of the electrodes. If the poling is done along the axial direction of the sensors with the electrodes on the upper and lower surfaces, the electric displacement is given by

$$D_3 = \overline{Q}_{55} d_{15} \gamma_{xz} = e_{15} \gamma_{xz}, \quad (67)$$

$$\mathbf{q} = \int_A e_{15}\left(\theta + \frac{\partial w_0}{\partial x}\right)\partial A \ , \quad (68)$$

where e_{15} is the piezoelectric constant. On solving Eqn. (68), we get

$$\mathbf{q}(t) = e_{15}\, c \frac{6\eta}{\left(-12\eta + l^2\right)}\begin{bmatrix} 0 & 2 & -l & 0 & -2 & -l \end{bmatrix}\begin{bmatrix} u_1 \\ w_1 \\ \theta_1 \\ u_2 \\ w_2 \\ \theta_2 \end{bmatrix}. \quad (69)$$

Here, $\begin{bmatrix} u_1 \\ w_1 \\ \theta_1 \\ u_2 \\ w_2 \\ \theta_2 \end{bmatrix} = \mathbf{q}$ is the vector of nodal displacements, i.e., the vector of axial displacement, transverse displacement and slopes at the fixed end and the free end. The current induced on the sensor surface is given by differentiating the total charge accumulated on the sensor surface and is given by

$$i(t) = \frac{d\,q(t)}{dt} = \dot{\mathbf{q}}(t) \quad (70)$$

or

$$\boldsymbol{i}(t) = e_{15}\, c \frac{6\eta}{\left(-12\eta + l^2\right)}\begin{bmatrix} 0 & 2 & -l & 0 & -2 & -l \end{bmatrix}\begin{bmatrix} \dot{u}_1 \\ \dot{w}_1 \\ \dot{\theta}_1 \\ \dot{u}_2 \\ \dot{w}_2 \\ \dot{\theta}_2 \end{bmatrix}. \quad (71)$$

Since the PE sensor is used as a strain rate sensor, this current can be converted into the open circuit sensor voltage $V^s(t)$ using a signal-conditioning device with a gain of G_c and applied to the actuator with the controller gain K_c.

$$V^s(t) = G_c\, \boldsymbol{i}(t), \quad (72)$$

$$V^s(t) = e_{15}\, c \frac{6\eta}{\left(-12\eta + l^2\right)} G_c \begin{bmatrix} 0 & 2 & -l & 0 & -2 & -l \end{bmatrix}[\dot{q}], \quad (73)$$

$$V^s(t) = \mathbf{p}^T \dot{\mathbf{q}}, \quad (74)$$

where $\dot{\mathbf{q}}$ is the time derivative of the modal coordinate vector (strain rate) and $\mathbf{p}^T$ is a constant vector which depends on the type of sensor and its finite element location in the embedded structure and is given by

$$\frac{6\eta e_{15}\, c G_c}{\left(-12\eta + L^2\right)}\begin{bmatrix} 0 & 2 & -L & 0 & -2 & -L \end{bmatrix}. \quad (75)$$

The input voltage to the actuator is $V^a(t)$ and is given by

$$V^a(t) = K_c\, V^s(t) \ , \quad (76)$$

$$V^a(t) = K_c \frac{6\eta e_{15}\, c G_c}{\left(-12\eta + L^2\right)}\begin{bmatrix} 0 & 2 & -L & 0 & -2 & -L \end{bmatrix}\dot{\mathbf{q}} \quad (77)$$

where K_c is the gain of the controller. The sensor output voltage is a function of the second spatial derivative of the mode shape.

2) Actuator Equation

The strain produced in the piezoelectric layer is directly proportional to the electric potential applied to the layer and is given by [6] [22]

$$\gamma_{xz} \propto E_f, \quad (78)$$

where γ_{xz} is the shear strain in the piezoelectric layer, and E_f is the electric potential applied to the actuator. From the constitutive piezoelectric equation, we get,

$$\gamma_{xz} = d_{15} E_f . \quad (79)$$

Since the ratio of shear stress to shear strain is the modulus of rigidity G, the shear stress is given by

$$\tau_{xz} = G \gamma_{xz} . \quad (80)$$

Substituting the value of γ_{xz} from Eqn. (79) into Eqn. (80) we get

$$\tau_{xz} = G d_{15} E_f \quad (81)$$

and

$$E_f = \frac{V^a(t)}{t_p}, \quad (82)$$

where t_p is the thickness of the piezoelectric layer. Thus,

$$\tau_{xz} = G d_{15} \frac{V^a(t)}{t_p} . \quad (83)$$

Because of the stress and strain, bending moments are induced in the beam at the nodes and the resultant moment M_a acting on the beam is determined by integrating the stress throughout the structure thickness as

$$M_a = G d_{15} V^a(t) \bar{h} = G d_{15} K_c \mathbf{p}^T \dot{\mathbf{q}} \bar{h} , \quad (84)$$

where $\bar{h} = \frac{(t_a + t_b)}{2}$ is the distance from the neutral axis of the beam and the piezoelectric layer. The work done by this moment results in the generation of the control force that is applied by the actuator as

$$\mathbf{f}_{ctrl} = G d_{15} \bar{h} \int_0^{l_p} N_\theta \, dx \, V^a(t) \quad (85)$$

or can be expressed as a scalar product

$$\mathbf{f}_{ctrl} = \mathbf{h} \, V^a(t) , \quad (86)$$

where $\mathbf{h}^T$ is a constant vector which depends on the type of actuator and its finite element location in the embedded structure and d_{15} is the piezoelectric strain constant. If any external forces described by the vector $\mathbf{f}_{ext}$ are acting then, the total force vector becomes

$$\mathbf{f}^t = \mathbf{f}_{ext} + \mathbf{f}_{ctrl} . \quad (87)$$

C. Dynamic equation of the smart structure

The dynamic equation of the smart structure is obtained by using both the regular beam elements and the embedded piezoelectric beam elements given in Eqns. (61) and (65). The beam is divided into 5 finite elements. Eqn. (61) and (65) gives the mass and stiffness of one of the regular beam elements which are called as the local mass matrix and the local stiffness matrix [30]-[32]. The mass and stiffness of the entire beam, which is divided into 5 finite elements is assembled using the FEM technique [35] and assembled matrices (global matrices), $\mathbf{M}$ and $\mathbf{K}$ is obtained [30]-[32]. The mass and stiffness matrices of the dynamic equation of the smart structure i.e., $\mathbf{M}$ and $\mathbf{K}$ include the sensor / actuator mass and stiffness. The equation of motion of the smart structure is given by

$$\mathbf{M}\ddot{\mathbf{q}} + \mathbf{K}\mathbf{q} = \mathbf{f}_{ext} + \mathbf{f}_{ctrl} = \mathbf{f}^t , \quad (88)$$

where $\mathbf{M}$ is the assembled mass matrix of the smart structure, $\mathbf{K}$ is the assembled stiffness matrix of the smart structure, $\mathbf{q}$ is the nodal variable vector and $\ddot{\mathbf{q}}$ is the acceleration vector.

The generalized coordinates are introduced in Eqn. (88) to reduce it further such that the resultant equation represents the dynamics of the desired number of modes of vibration and the uncoupled equations are obtained [23] - [25], [29]. Let the transformation for this purpose used be

$$\mathbf{q} = \mathbf{T}\,\mathbf{g} , \quad (89)$$

where $\mathbf{T}$ is the modal matrix containing the eigenvectors representing the desired number of modes of vibration of the cantilever beam. This method is used to derive the uncoupled equations governing the motion of the free vibrations of the system in terms of principal coordinates by introducing a linear transformation between the generalized coordinates $\mathbf{q}$ and the principal coordinates $\mathbf{g}$. The equation (88) after applying the transformation and multiplying by $\mathbf{T}^T$ on both sides and further simplifying becomes

$$\mathbf{M}^* \ddot{\mathbf{g}} + \mathbf{K}^* \mathbf{g} = \mathbf{f}_{ext}^* + \mathbf{f}_{ctrl}^* , \quad (90)$$

where the matrices $\mathbf{M}^*, \mathbf{K}^*, \mathbf{f}_{ext}^*$ and $\mathbf{f}_{ctrl}^*$ are the generalized mass matrix, the generalized damping matrix, the generalized external force vector and the generalized control force vector and given by

$$\mathbf{M}^* = \mathbf{T}^T \mathbf{M} \mathbf{T} , \quad (91)$$

$$\mathbf{T}^* = \mathbf{T}^T \mathbf{K} \mathbf{T} , \quad (92)$$

$$\mathbf{f}_{\text{ext}}^{\ *} = \mathbf{T}^T \mathrm{f}_{ext} , \quad (93)$$

$$\mathbf{f}_{\text{ctrl}}^{\ *} = \mathbf{T}^T \mathrm{f}_{ctrl} . \quad (94)$$

The structural damping matrix is introduced into Eqn. (90) by using

$$\mathbf{C}^* = \alpha \mathbf{M}^* + \beta \mathbf{K}^* \quad (95)$$

where $\mathbf{C}^*$ is the generalized damping matrix (also called as Rayleigh damping), which is of the form given in Eqn. (95), α and β being the structural constants. α and β are determined from 3 given damping ratios that correspond to three unequal frequencies of vibration. The dynamic equation of the smart structure finally, is given by [36]

$$\mathbf{M}^* \ddot{\mathbf{g}} + \mathbf{C}^* \dot{\mathbf{g}} + \mathbf{K}^* \mathbf{q} = \mathbf{f}_{ext}^* + \mathbf{f}_{ctrl}^* . \quad (96)$$

Note that the dynamic equation decouples the equations corresponding to each individual mode, provided the damping is proportional as described by Eqn. (95).

D. State Space Model of the Smart Structure

The governing equation in (96) is written in the state space form and is obtained as below. Let the transformation used be

$$\mathbf{g} = \mathbf{x}, \tag{97}$$

where

$$\mathbf{g} = \begin{bmatrix} g_1 \\ g_2 \\ g_3 \end{bmatrix} = \begin{bmatrix} x_1 \\ x_2 \\ x_3 \end{bmatrix} = \mathbf{x}. \tag{98}$$

Now,

$$\dot{\mathbf{g}} = \dot{\mathbf{x}} = \begin{bmatrix} \dot{g}_1 \\ \dot{g}_2 \\ \dot{g}_3 \end{bmatrix} = \begin{bmatrix} \dot{x}_1 \\ \dot{x}_2 \\ \dot{x}_3 \end{bmatrix} = \begin{bmatrix} x_4 \\ x_5 \\ x_6 \end{bmatrix} \tag{99}$$

and

$$\ddot{\mathbf{g}} = \ddot{\mathbf{x}} = \begin{bmatrix} \dot{x}_4 \\ \dot{x}_5 \\ \dot{x}_6 \end{bmatrix}. \tag{100}$$

Thus,

$$\begin{aligned} \dot{x}_1 &= x_4, \\ \dot{x}_2 &= x_5, \\ \dot{x}_3 &= x_6 \end{aligned} \tag{101}$$

and Eqn. (96) now becomes

$$\mathbf{M}^* \begin{bmatrix} \dot{x}_4 \\ \dot{x}_5 \\ \dot{x}_6 \end{bmatrix} + \mathbf{C}^* \begin{bmatrix} x_4 \\ x_5 \\ x_6 \end{bmatrix} + \mathbf{K}^* \begin{bmatrix} x_1 \\ x_2 \\ x_3 \end{bmatrix} = \mathbf{f}^*_{ext} + \mathbf{f}^*_{ctrl}. \tag{102}$$

which is further simplified as

$$\begin{bmatrix} \dot{x}_4 \\ \dot{x}_5 \\ \dot{x}_6 \end{bmatrix} = -\mathbf{M}^{*-1}\mathbf{K}^* \begin{bmatrix} x_4 \\ x_5 \\ x_6 \end{bmatrix} - \mathbf{M}^{*-1}\mathbf{C}^* \begin{bmatrix} x_1 \\ x_2 \\ x_3 \end{bmatrix} + \mathbf{M}^{*-1}\mathbf{f}^*_{ext} + \mathbf{M}^{*-1}\mathbf{f}^*_{ctrl}. \tag{103}$$

The generalized external force coefficient vector is

$$\mathbf{f}^*_{ext} = \mathbf{T}^T \mathbf{f}_{ext} = \mathbf{T}^T f\, r(t), \tag{104}$$

where $r(t)$ is the external force input to the beam.

The generalized control force coefficient vector is

$$\mathbf{f}^*_{ctrl} = \mathbf{T}^T f_{ctrl} = \mathbf{T}^T \mathbf{h}\, V^a(t) = \mathbf{T}^T \mathbf{h}\, u(t), \tag{105}$$

where the voltage $V^a(t)$ is the input voltage to the actuator from the controller and is nothing but the control input $u(t)$ to the actuator and $\mathbf{h}$ is a constant vector which depends on the actuator type and its finite element location in the embedded structure. So, using the Eqns. (101), (104) and (105) in Eqn. (103), the state space equation for the smart beam is represented as

$$\begin{bmatrix} \dot{x}_1 \\ \dot{x}_2 \\ \dot{x}_3 \\ \dot{x}_4 \\ \dot{x}_5 \\ \dot{x}_6 \end{bmatrix} = \begin{bmatrix} 0 & I \\ -\mathbf{M}^{*-1}\mathbf{K}^* & -\mathbf{M}^{*-1}\mathbf{C}^* \end{bmatrix}_{(6\times 6)} \begin{bmatrix} x_1 \\ x_2 \\ x_3 \\ x_4 \\ x_5 \\ x_6 \end{bmatrix} + \begin{bmatrix} 0 \\ \mathbf{M}^{*-1}\mathbf{T}^T\mathbf{h} \end{bmatrix}_{(6\times 1)} \mathbf{u}(t) + \begin{bmatrix} 0 \\ \mathbf{M}^{*-1}\mathbf{T}^T\mathbf{f} \end{bmatrix}_{(6\times 1)} r(t), \tag{106}$$

where $u(t)$ is the control input, $r(t)$ is the external input to the system, $\mathbf{f}$ is the external force coefficient vector. The sensor equation is modeled as

$$V^s(t) = \mathbf{p}^T \dot{\mathbf{q}} = y(t), \tag{107}$$

where $\mathbf{p}^T$ is a constant vector which depends on the piezoelectric sensor characteristics (i.e., the sensor constant) and on the position of the sensor location in the embedded beam structure. Thus, the sensor output for a SISO case is given by

$$y(t) = \mathbf{p}^T \dot{\mathbf{q}} = \mathbf{p}^T \mathbf{T} \dot{\mathbf{g}} = \mathbf{p}^T \mathbf{T} \begin{bmatrix} x_4 \\ x_5 \\ x_6 \end{bmatrix}, \tag{108}$$

which can be written in the state space form as

$$y(t) = \begin{bmatrix} 0 & \mathbf{p}^T\mathbf{T} \end{bmatrix}_{(1\times 6)} \begin{bmatrix} x_1 \\ x_2 \\ x_3 \\ x_4 \\ x_5 \\ x_6 \end{bmatrix}. \tag{109}$$

Thus, the state space model of the smart system, i.e., the state space equation and the output equation is given by

$$\begin{aligned} \dot{\mathbf{x}} &= \mathbf{A}\,\mathbf{x}(t) + \mathbf{B}\,\mathbf{u}(t) + \mathbf{E}\,\mathbf{r}(t), \\ y(t) &= \mathbf{C}^T\,\mathbf{x}(t) \end{aligned} \tag{110}$$

with

$$\mathbf{A} = \begin{bmatrix} 0 & I \\ -\mathbf{M}^{*-1}\mathbf{K}^* & -\mathbf{M}^{*-1}\mathbf{C}^* \end{bmatrix}_{(6\times 6)}, \tag{111}$$

$$\mathbf{B} = \begin{bmatrix} \mathbf{0} \\ \mathbf{M}^{*-1}\mathbf{T}^T\mathbf{h} \end{bmatrix}_{(6\times 1)}, \tag{112}$$

$$\mathbf{C}^T = \begin{bmatrix} 0 & \mathbf{p}^T \end{bmatrix}_{(1\times 6)}, \tag{113}$$

$$\mathbf{D} = \text{Null Matrix}, \tag{114}$$

$$\mathbf{E} = \begin{bmatrix} 0 \\ \mathbf{M}^{*-1}\mathbf{T}^{T}\mathbf{f} \end{bmatrix}_{(6\times 1)}, \quad (115)$$

where $r(t), u(t), \mathbf{A}, \mathbf{B}, \mathbf{C}, \mathbf{D}, \mathbf{E}, x(t)$ and $y(t)$ represents the external force input, the control input, system matrix, input matrix, output matrix, transmission matrix, external load matrix, state vector, system output (sensor output). The values of the $\mathbf{A}, \mathbf{B}, \mathbf{C}, \mathbf{D}, \mathbf{E}$ matrices for the model 1 with actuator at FE 1 and sensor at FE 2 of the smart structure is given by

$$\mathbf{A} = 1e5 \begin{bmatrix} 0 & 0 & 0 & 0.00001 & 0 & 0 \\ 0 & 0 & 0 & 0 & 0.00001 & 0 \\ 0 & 0 & 0 & 0 & 0 & 0.00001 \\ -1.06 & -0.00 & 0.00 & -0.00 & -0.00 & 0.00 \\ -0.00 & -3.73 & 0.00 & -0.00 & -0.00 & -0.00 \\ 0.00 & -0.00 & -0.00 & 0.00 & -0.00 & -0.0001 \end{bmatrix}, \quad (116)$$

$$\mathbf{B} = 1e-4 \begin{bmatrix} 0 \\ 0 \\ 0 \\ 0.2346 \\ -0.0000 \\ -0.8647 \end{bmatrix}, \quad (117)$$

$$\mathbf{C}^{T} = \begin{bmatrix} 0 & 0 & 0 & -0.0001 & 0.0000 & 0.0014 \end{bmatrix}, \quad (118)$$

$$\mathbf{D} = \text{Null matrix}, \quad (119)$$

$$\mathbf{E} = \begin{bmatrix} 0 \\ 0 \\ 0 \\ -4.9470 \\ 0.0000 \\ 1.5310 \end{bmatrix}. \quad (120)$$

Similarly, the state space models of the remaining 3 models are obtained. By making one pair of piezoelectric elements as non-collocated active sensors / actuator at a time and by making other elements as regular elements, control of this SISO state space model is obtained using the fast output sampling feedback control technique which is considered in the next section. The characteristics of the smart flexible SISO cantilever beam are given in Table III.

TABLE III
CHARACTERISTICS OF THE SMART FLEXIBLE SISO BEAM

Eigen values	3 Natural Freq. (Hz)
$-0.5344 \pm j\,326.92$	52.0312
$-1.8648 \pm j\,610.71$	97.1970
$-4.1968 \pm j\,916.16$	145.8111

IV. Design of the Fast Output Sampling Feedback Controller

The control problem is as follows **:** Developing of the control strategy for the SISO representation of the developed smart structure model using fast output sampling feedback control law [20] [21].

A. Review of the fast output sampling feedback control technique

A standard result in control theory says that the poles of a LTI controllable system can be arbitrarily assigned by state feedback. In many cases, the entire state vector is not directly available for feedback purposes. Hence, it is desirable to go for an output feedback design. The static output feedback problem is one of the most investigated problems in the control theory and applications [19].

One reason why the static output feedback has received so much attention is that it represents the simplest closed loop control that can be realized in practical situations. However, no results are available till today which show that complete pole assignment is possible using static output feedback. Practicing state feedback and optimal output feedback controllers needs careful consideration in smart structure application area like the space structures, because the state feedback controller needs the availability of the entire state vector or need estimator.

In the state feedback case, the optimal control law requires the design of a state observer. This increases the implementation cost and reduces the reliability of the control system. Another disadvantage of the observer based control system is that even slight variations of the model parameters from their nominal values may result into significant degradation of the closed-loop performance.

The static output feedback requires only the measurement of the system output, but there is no guarantee of the stability of the closed loop control system. Although the stability of the closed loop system can be guaranteed using the state feedback, the same is not true using static output feedback. So, if a system, for example, smart cantilever beam, in this case, has to be stabilized using only the output feedback (states may not be available for measurement purposes), one can resort to fast output sampling feedback, which is static in nature as well, guarantees the closed loop stability. Here, the value of the input at a particular moment depends on the output value at a time prior to this moment (namely at the beginning of the period).

The problem of fast output sampling was studied by Werner and Furuta [20], [21] for linear time invariant systems with infrequent observations. They have shown that the poles of the discrete time control system could be assigned arbitrarily (within the natural restriction that they should be located symmetrically with respect to the real axis) using the fast output sampling technique. Since the feedback gains are piecewise constants, their method could easily be implemented and indicated a new possibility. Such a control law can stabilize a much larger class of systems.

Consider a plant described by a LTI state space model given by

$$\dot{x}(t) = A\,x(t) + B\,u(t), \qquad y(t) = C\,x(t). \tag{121}$$

where $x \in \Re^n$, $x \in \Re^m$, $x \in \Re^p$, $A \in \Re^{n\times n}$, $B \in \Re^{n\times m}$, $C \in \Re^{p\times n}$, A, B, C are constant matrices and it is assumed that (A,B) is controllable and (C,A) is observable. Assume that output measurements are available at time instants $t = k\,\tau$, where $k = 0,1,2,3,....$ Now, construct a discrete linear time invariant system from these output measurements at sampling rate $\frac{1}{\tau}$ (sampling interval of τ secs). The system obtained so is called as the τ system and is given by

$$x((k+1)\,\tau) = \Phi_\tau\, x(k\tau) + \Gamma_\tau\, u(k\tau), \qquad y(k\tau) = C\,x(k\tau), \tag{122}$$

where $\Phi_\tau, \Gamma_\tau, C$ are constant matrices of appropriate dimensions. Assume that the plant is to be controlled by a digital computer, with sampling interval τ and zero order hold and that a sampled data state feedback design has been carried out to find a state feedback gain F such that the closed loop system

$$x(k\tau + \tau) = (\Phi_\tau + \Gamma_\tau F)\,x(k\tau) \tag{123}$$

has desirable properties. Here,

$$\Phi_\tau = e^{A\tau} \tag{124}$$

and

$$\Gamma_\tau = \int_0^\tau e^{As}\,ds\,B\,. \tag{125}$$

Instead of using a state observer, the following sampled data control can be used to realize the effect of the state feedback gain F by output feedback. Let $\Delta = \frac{\tau}{N}$ and consider

$$u(t) = \begin{bmatrix} L_0 & L_1 & ..... & L_{N-1} \end{bmatrix} \begin{bmatrix} y(k\tau - \tau) \\ y(k\tau - \tau + \Delta) \\ : \\ : \\ y(k\tau - \Delta) \end{bmatrix}, \tag{126}$$

i.e.,

$$u(t) = L\ y_k \tag{127}$$

for $k\tau \le t \le (k+1)\tau$, where the matrix blocks L_j represent the output feedback gains and the notation L, y_k has been introduced for convenience. Note that $\frac{1}{\tau}$ is the rate at which the loop is closed, whereas the output samples are taken at the times N - times faster rate $\frac{1}{\Delta}$. This control law is illustrated in the Fig. 4.

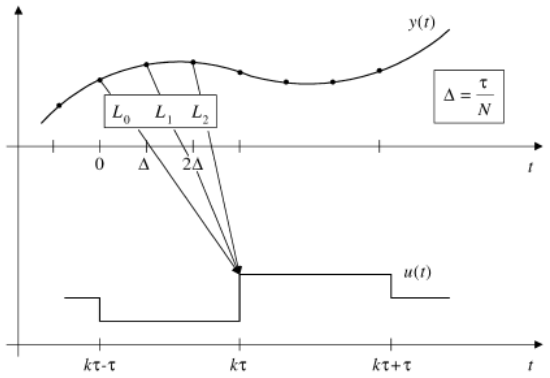

Fig. 4 Graphical illustration of fast output sampling feedback method

To show how a fast output sampling controller in Eqn. (127) can be designed to realize the given sampled data state feedback gain for a controllable and observable system (A,B,C), we construct a fictitious, lifted system for which the Eqn. (126) can be interpreted as static output feedback [19]. Let (Φ,Γ,C) denote the system in Eqn. (121) sampled at the rate $\frac{1}{\Delta}$ and is called as the delta system. Consider the discrete time system having at time $t = k\tau$, the input $u_k = u(k\tau)$, the state $x_k = x(k\tau)$ and the output y_k as

$$x_{k+1} = \Phi_\tau x_k + \Gamma_\tau u_k, \qquad y_{k+1} = \mathbf{C}_0 x_k + \mathbf{D}_0 u_k, \tag{128}$$

where

$$\mathbf{C}_0 = \begin{bmatrix} C \\ C\Phi \\ \vdots \\ C\Phi^{N-1} \end{bmatrix}, \quad \mathbf{D}_0 = \begin{bmatrix} 0 \\ C\Gamma \\ \vdots \\ C\sum_{j=0}^{N-2} \Phi^j\,\Gamma \end{bmatrix}. \tag{129}$$

Assume that the state feedback gain F has been designed such that $(\Phi_\tau + \Gamma_\tau F)$ has no eigen values at the origin. Then, assuming that in the interval $k\tau \le t \le (k\tau + \tau)$,

$$u(t) = F\,x(k\tau), \tag{130}$$

one can define the fictitious measurement matrix,

$$\mathbf{C}(F,N) = (\mathbf{C}_0 + \mathbf{D}_0 F)(\Phi_\tau + \Gamma_\tau F)^{-1}, \tag{131}$$

which satisfies the fictitious measurement equation

$$y_k = \mathbf{C}\,x_k\,. \tag{132}$$

For $\mathbf{L}$ to realize the effect of F, it must satisfy [20], [21], [25] the equation

$$\mathbf{L}\mathbf{C} = F\,. \tag{133}$$

Let υ denote the observability index of (Φ, Γ, C). It can be shown that for $N \geq \upsilon$, generically $\mathbf{C}$ has full column rank, so that any state feedback gain can be realized by a fast output sampling gain $\mathbf{L}$. If the initial state is unknown, there will be an error $\Delta u_k = u_k - F x_k$ in constructing the control signal under the state feedback. One can verify that the closed-loop dynamics are governed by [20], [21], [25].

$$\begin{bmatrix} x_{k+1} \\ \Delta u_{k+1} \end{bmatrix} = \begin{bmatrix} \Phi_\tau + \Gamma_\tau F & \Gamma_\tau \\ 0 & \mathbf{L}\mathbf{D}_0 - \Gamma_\tau \end{bmatrix} \begin{bmatrix} x_k \\ \Delta u_k \end{bmatrix}. \quad (134)$$

To see this, apply the coordinate transformation,

$$T = \begin{bmatrix} I & 0 \\ F & I \end{bmatrix} \quad (135)$$

to the equation

$$\begin{bmatrix} x_{k+1} \\ u_{k+1} \end{bmatrix} = \begin{bmatrix} \Phi_\tau & \Gamma_\tau \\ \mathbf{L}\mathbf{C}_0 & \mathbf{L}\mathbf{D}_0 \end{bmatrix} \begin{bmatrix} x_k \\ \Delta u_k \end{bmatrix} \quad (136)$$

and use Eqn. (131). Thus, one can say that the eigen-values of the closed-loop system under a fast output sampling control law given in Eqn. (131) are those of $(\Phi_\tau + \Gamma_\tau F)$ together with those of $(\mathbf{L}\mathbf{D}_0 - \Gamma_\tau)$. This suggests that the state feedback F should be obtained so as to ensure the stability of both $(\Phi_\tau + \Gamma_\tau F)$ and $(\mathbf{L}\mathbf{D}_0 - F\Gamma_\tau)$. The system in Eqn. (128) is stable if and only if F stabilizes (Φ_τ, Γ_τ) and the matrix $(\mathbf{L}\mathbf{D}_0 - F\Gamma_\tau)$ has all its eigen values inside the unit circle. The problem with controllers obtained in this way is that, although they are stabilizing and achieve the desired closed loop behavior in the output sampling instants, they may cause an excessive oscillation between sampling instants. The fast output sampling feedback gains obtained may be very high. To reduce this effect, we relax the condition that L exactly satisfy the linear equation (133) and include a constraint on the gain L. Thus, we arrive at the following in Eqns. (137)-(140).

$$\|L\| < \rho_1, \ \|\mathbf{L}\mathbf{D}_0 - F\Gamma_\tau\| < \rho_2, \ \|\mathbf{L}\mathbf{C} - F\| < \rho_3. \quad (137)$$

This can be formulated in the form of Linear Matrix Inequalities (LMI's) as

$$\begin{bmatrix} -\rho_1^{\,2} I & \mathbf{L} \\ \mathbf{L}^T & -I \end{bmatrix} < 0, \quad (138)$$

$$\begin{bmatrix} -\rho_2^{\,2} I & \mathbf{L}\mathbf{D}_0 - F\Gamma_\tau \\ (\mathbf{L}\mathbf{D}_0 - F\Gamma_\tau)^T & -I \end{bmatrix} < 0, \quad (139)$$

$$\begin{bmatrix} -\rho_3^{\,2} I & \mathbf{L}\mathbf{C} - F \\ (\mathbf{L}\mathbf{C} - F)^T & -I \end{bmatrix} < 0. \quad (140)$$

In this form, the LMI optimization toolbox is used for the synthesis of L [7].

B. FOS Controller Design for the SISO beam

The FEM model of the smart cantilever beam based on Laminate Beam Theory is developed using MATLAB. Different state space models of the smart cantilever beam are obtained by keeping the actuator location fixed (i.e., at fixed end) and varying the position of the sensor from the nearby fixed end to the free end. A fast output sampling feedback controller discussed in the previous section is designed to suppress the first three modes of vibration of the smart cantilever beam. All simulations are done using MATLAB. The performance of the beam is evaluated for vibration control with the proposed control technique.

The first task in designing the fast output sampling feedback controller is the selection of the sampling interval τ. The maximum bandwidth for the sensor / actuator locations on the beam are calculated (here, the third vibratory mode of the plant). Then, by using the existing empirical rules for selecting the sampling interval based on bandwidth, approximately 10 times of the maximum third vibration mode frequency of the system is selected. The sampling interval τ used is 0.004 secs.

Four different configurations of the beam are considered. In all the four cases, the length of the beam is 30 cm and its cross section is 1 mm by 2 cm. The length of the peizo patch is 6 cm and its cross section is 1 mm by 2 cm. The material properties used for the generation of the FEM model are given in Table I and II respectively. A sixth order state space model of the system is obtained on retaining the first three modes of vibration of the system as shown in Section 3. The first three natural frequencies obtained are 52.03 Hz, 97.21 Hz and 145.81 Hz.

In the first case, the FEM model of the smart cantilever beam is obtained by dividing the beam into 5 elements. The actuator is placed as the 1st element (at the fixed end) and the sensor is placed as the 2nd finite element as shown in Fig. 5.

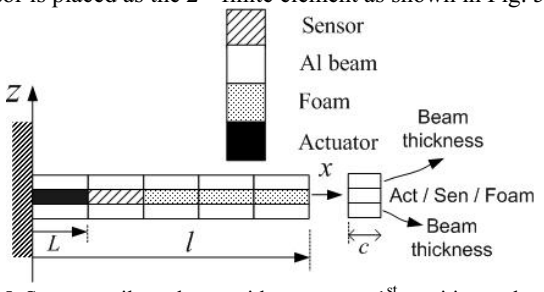

Fig. 5 Smart cantilever beam with actuator at 1st position and sensor at 2nd position

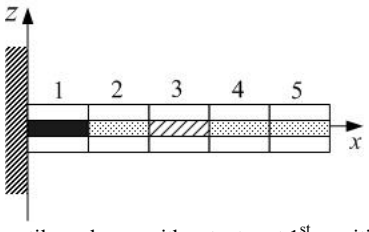

Fig. 6 Smart cantilever beam with actuator at 1st position and sensor at 3rd position

In the second case, the FEM model of the smart cantilever beam is obtained by dividing the beam into 5 elements and placing the actuator at the 1st finite element location and the sensor at the 3rd finite element location as shown in Fig. 6.

In the third case, the FEM model of the smart cantilever beam is obtained by dividing the beam into 5 elements and placing the actuator at the 1st finite element location and the sensor at the 4th finite element location as shown in Fig. 7.

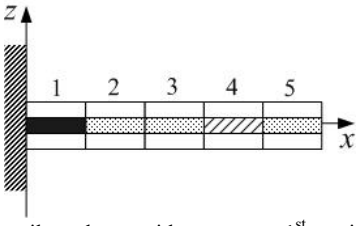

Fig. 7 Smart cantilever beam with actuator at 1st position and sensor at 4th position

In the fourth case, the FEM model of the smart cantilever beam is obtained by dividing the beam into 5 elements and placing the actuator at the 1st finite element location and the sensor at the 5th finite element location as shown in Fig. 8.

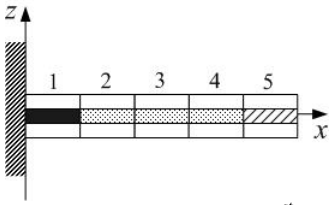

Fig. 8 Smart cantilever beam with actuator at 1st position and sensor at 5th position

A external force $\mathbf{f}_{ext}$ (impulse disturbance) of 1 Newton is applied for a duration of 50 ms at the free end of the beam for the systems shown in Figs. 5 to 8 and the open loop impulse responses (without control) of the system are observed. Controllers based on the fast output sampling feedback control algorithm are designed to control the first three modes of vibration of the smart cantilever beam with embedded shear sensor and actuator for the systems shown in Figs. 5 to 8. The sampling interval used is 0.004 secs and is divided into 10 subintervals $(N=10)$.

Let $(\Phi_{\tau i}, \Gamma_{\tau i}, C_i)$ with i = 1 to 4 be the discrete time systems (tau system) of the systems in Fig. 1 in Eqn. (110) sampled at a rate of $1/\tau$ seconds respectively. It is found that the tau systems are controllable and observable and are given by

$$\Phi_{\tau 1}=\begin{bmatrix} 0.26 & -0.00 & 0.00 & 0.002 & -0.00 & 0.00 \\ -0.0 & -0.75 & -0.00 & -0.00 & 0.001 & -0.00 \\ 0.00 & -0.00 & -0.85 & 0.00 & -0.00 & -0.0005 \\ -314.9 & -0.00 & -0.00 & 0.25 & -0.00 & 0.00 \\ -0.0 & -389.9 & 0.00 & -0.00 & -0.76 & -0.00 \\ -0.0 & 0.00 & 450.02 & 0.00 & -0.00 & -0.85 \end{bmatrix}, \quad (141)$$

$$\Gamma_{\tau 1}=1.0\text{e-}7*\begin{bmatrix} 0.0016 \\ -0.0000 \\ -0.0019 \\ 0.6915 \\ -0.0000 \\ 0.4636 \end{bmatrix}, \quad (142)$$

$$\mathbf{C}_1^{\,T}=[0 \quad 0 \quad 0 \quad -0.0001 \quad 0.0000 \quad 0.0014], \quad (143)$$

for the tau system of the SISO model 1. Similarly, the tau systems for other 3 models are obtained. The stabilizing state feedback gains are obtained for each of the tau systems such that the eigenvalues of $(\Phi_{\tau i}+\Gamma_{\tau i}F_i)$ lie inside the unit circle and the response of the system has a good settling time. The state feedback gains obtained are as

$$F_1=[-2.0322 \quad 0.0000 \quad 0.0024 \quad 0.0081 \quad -0.0000 \quad 0.0000] \quad (85)$$

for the model 1. Similarly, the state feedback gains for the other three models are obtained. The closed loop impulse response of the 4 models of the system with the state feedback gain F is also observed.

Let (Φ, Γ, C) be the discrete time systems (delta system) of the system in Fig. 1 in Eqn. (110) sampled at the rate $1/\Delta$ secs respectively, where $\Delta=\tau/N$. The delta system for the SISO model 1 is given by

$$\Phi_1=\begin{bmatrix} 0.99 & -0.00 & 0.00 & 0.0004 & -0.00 & 0.00 \\ 0.00 & 0.97 & 0.00 & -0.00 & 0.0004 & 0.00 \\ 0.00 & 0.00 & 0.96 & 0.00 & -0.00 & -0.0003 \\ -42.6 & 0.00 & -0.00 & 0.99 & -0.00 & -0.00 \\ -0.0 & -147.6 & -0.00 & -0.00 & 0.96 & 0.00 \\ 0.00 & 0.00 & 236.8 & 0.00 & 0.00 & 0.96 \end{bmatrix}, \quad (144)$$

$$\Gamma_1=-1.0\text{e}-7*\begin{bmatrix} 0.0000 \\ -0.0000 \\ -0.0000 \\ 0.0936 \\ 0.0000 \\ 0.2440 \end{bmatrix}, \quad (145)$$

$$\mathbf{C}_1^{\,T}=[0 \quad 0 \quad 0 \quad -0.0001 \quad 0.0000 \quad 0.0014], \quad (146)$$

Similarly, the delta systems for the other 3 SISO models are obtained. The fast output sampling feedback gain matrix $\mathbf{L}$ for the system given in Eqns. (101) and (105) is obtained by solving $\mathbf{LC}=F$ using the LMI optimization method [7], [25] as

$$\mathbf{L}_1=[0.1111 \ 0.0734 \ 0.039 \ 0.0095 \ -0.038 \ .....$$
$$....-0.0304 \ -0.0403 \ -0.0440 \ -0.0426 \ -0.0377 \ ]. \quad (147)$$

Similarly, the FOS feedback gains are obtained for the other 3 models of the smart structure plant. The closed loop impulse responses (sensor outputs y) of all the models with

fast output sampling feedback gain $\mathbf{L}$ of the system is observed. Also, the variation of the control signal u with time for the systems is observed and the conclusions are drawn.

V. Simulation Results

In this section, we present the simulation results of the 4 SISO models. The following figures (Figs. 9 - 12) shows the open loop response, closed loop response with state feedback gain F, the closed loop response with the FOS feedback gain $\mathbf{L}$ and the magnitude of the control input u with time t for the smart cantilever beam with actuator at the first position and sensor location varied from second finite element position to the fifth finite element position. The comparisons of the quantitative results of the OL and CL responses (with state feedback gain F, FOS gain $\mathbf{L}$) and with the magnitude of the control efforts, their settling times required is shown in Table IV.

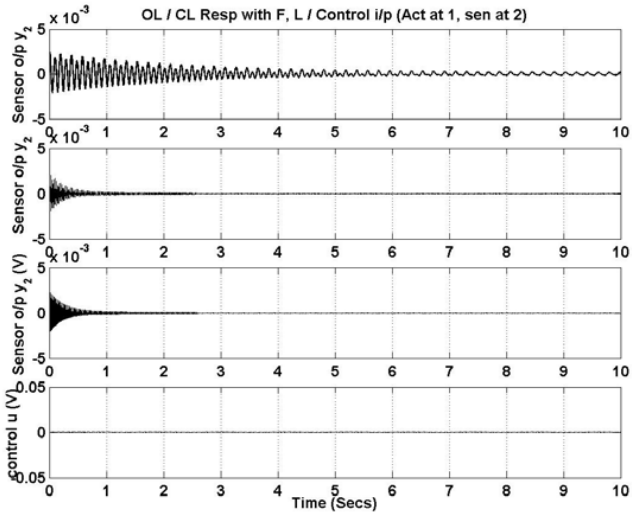

Fig. 9 OL / CL response with F and L / control u for model 1

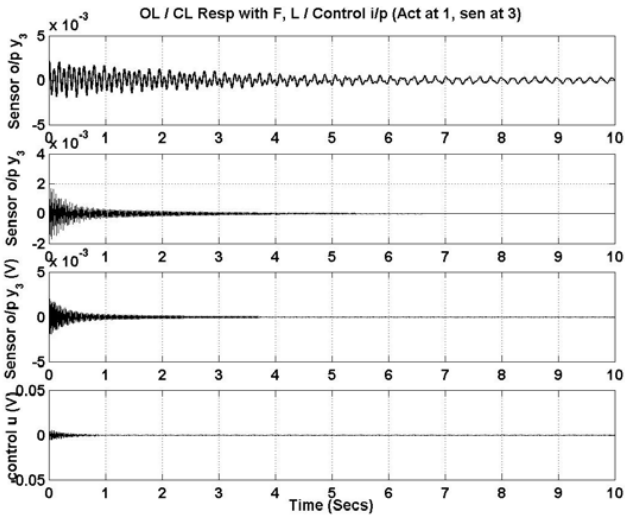

Fig. 10 OL / CL response with F and L / control u for model 2

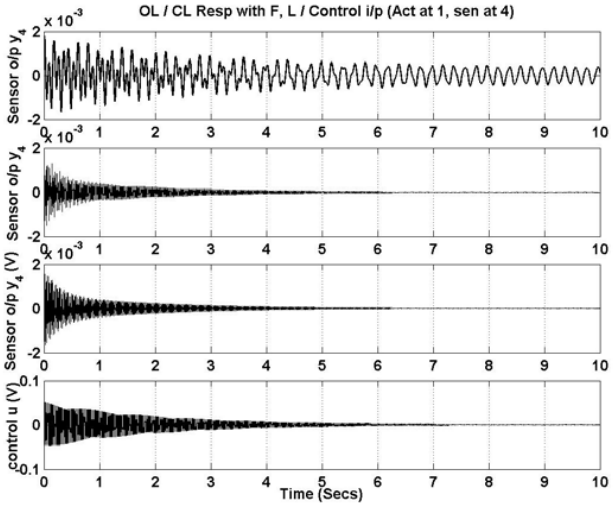

Fig. 11 OL / CL response with F and L / control u for model 3

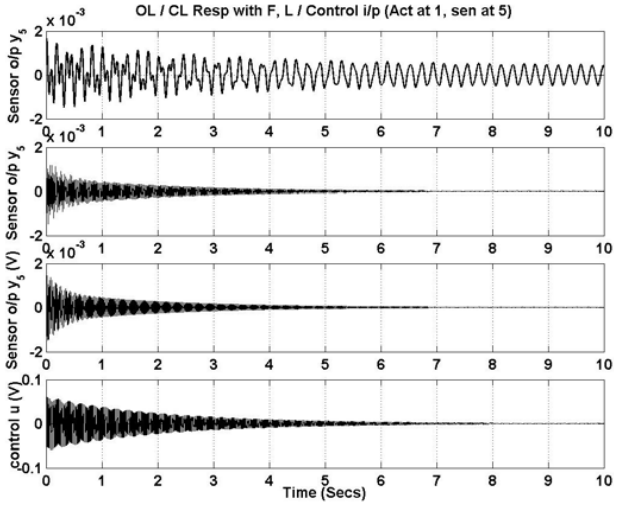

Fig. 12 OL / CL response with F and L / control u for model 4

TABLE IV
Quantitative comparitive results of the FOS simulations
[terms inside the brackets indicate settling times]

Model	Open loop	Closed loop with F	Closed loop with L	Control input u
1.	10 mV (11 secs)	25 mV (5 secs)	25 mV (4 secs)	0.005 V
2.	22 mV (15 secs)	22 mV (6 mV)	22 mV (5 secs)	0.01 V
3.	20 mV (19 sec)	19 mV (7 secs)	19 mV (6 secs)	0.05 V
4.	18 mV (22 secs)	(18 mV) (secs)	18 mV (7 secs)	0.06 V

VI. Conclusions

A Finite Element model of a smart cantilever beam based on Timoshenko Beam Theory with embedded piezoelectric

shear sensors and actuators is presented for the SISO representation of the smart structure in this research paper. Some of the limitations of Euler-Bernoulli beam theory, such as the axial displacement and the shear are being considered in this work.

Different smart cantilever beam models with embedded shear sensors / actuators are developed using the Timoshenko beam theory for different sensor locations keeping the actuator location fixed. A Fast Output Sampling feedback (FOS) controller is designed to control the first three modes of vibration of the embedded shear piezoelectric system. In the SISO case, four different models have been considered. The performance of the controller is evaluated for different sensor locations while the position of the sensor is kept constant.

It can be inferred from the response characteristics and the simulation results that the magnitude of the control signal u increases as the position of the sensor is changed from the nearby fixed end and moved towards the free end of the smart cantilever beam. The closed loop responses take more time to settle, i.e., for the vibrations to get damped out. The impulse responses with $\mathbf{L}$ and F show better performance when the sensor is at the nearby fixed end. Thus, it can be inferred from the simulation results, that when the plant is placed with this controller, the system performs well and stability is guaranteed.

It is also observed that the maximum amplitude of the control voltage required to dampen out the vibrations is less when the sensor is placed at FE position 2 than at the fixed end and also the response settles quicker and the vibrations are damped out quickly. From the Fig. 9-12, it can be inferred that without control the transient response is predominant and with control, the vibrations are suppressed. It is also observed from the simulation results that modeling a smart structure by including the sensor / actuator mass and stiffness and by varying the sensor location at different positions introduces a considerable change in the structural vibration characteristics.

The state feedback gain F for the SISO plant is obtained so that its poles are not placed at the origin and has a good settling time of less than 10 seconds. The designed FOS controller requires constant gains and hence is easier to implement in real time. The simulation results show that a fast output sampling feedback controller based on Timoshenko Beam Theory is able to satisfactorily control the first three modes of vibration of the smart cantilever beam.

Surface mounted piezoelectric collocated sensors and actuators (piezo-patches bonded to the master structure at top and bottom of the single flexible beam) are usually placed at the extreme thickness position of the structure (near by the fixed end) to achieve most effective sensing and actuation [25]. This subjects the sensors / actuators to high longitudinal stresses that might damage the brittle piezo-electric material. Furthermore, surface mounted sensors / actuators are likely to be damaged by contact with surrounding objects piezopatches coming out while vibrating, connections coming out, due to thermal effects, stray magnetic fields, noise signals, etc.,. embedded shear sensors / actuators can be used to alleviate these problems. The limitations of Euler-Bernoulli beam theory such as the neglection of the shear ϕ and axial displacements have been considered here while modeling the beam. Timoshenko beam theory corrects the simplifying assumptions made in Euler-Bernoulli beam theory and the model obtained can be a exact one.

ACRONYMS / ABBREVIATIONS

SISO	Single Input Single Output
FEM	Finite Element Method
FE	Finite Element
LMI	Linear Matrix Inequalities
MR	Magneto Rheological
ER	Electro Rheological
PVDF	Poly Vinylidene Fluoride
SMA	Shape Memory Alloys
CF	Clamped Free
CC	Clamped Clamped
CT	Continuous Time
DT	Discrete Time
OL	Open Loop
CL	Closed Loop
HOBT	Higher Order Beam Theory
RHS	Right Hand Side
LTI	Linear Time Invariant
FOS	Fast Output Sampling
AVC	Active Vibration Control
EB	Euler-Bernoulli
PZT	Lead Zirconate Titanate
DOF	Degree Of Freedom
IEEE	Institute of Electrical & Electronics Engineers
IOP	Institute of Physics
ISSS	Institute of Smart Structures and Systems
SPIE	Society of Photonics & Instrumentation Engineers

APPENDIX

The stiffness matrix for the sandwich beam element is obtained using the Eqn. (65) as

$$[K] = \begin{bmatrix} K_{11} & K_{12} & K_{13} & K_{14} & K_{15} & K_{16} \\ K_{21} & K_{22} & K_{23} & K_{24} & K_{25} & K_{26} \\ K_{31} & K_{32} & K_{33} & K_{34} & K_{35} & K_{36} \\ K_{41} & K_{42} & K_{43} & K_{44} & K_{45} & K_{46} \\ K_{51} & K_{52} & K_{53} & K_{54} & K_{55} & K_{56} \\ K_{61} & K_{62} & K_{63} & K_{64} & K_{65} & K_{66} \end{bmatrix},$$

where

$$K_{11} = \frac{AA_{11}}{L},\ K_{12} = K_{21} = \frac{AB_{11}}{L},\ K_{13} = K_{31} = 0$$

$$K_{14} = K_{41} = -\frac{AA_{11}}{L},\ K_{15} = K_{51} = -\frac{AB_{11}}{L}$$

$$K_{16} = K_{61} = 0,\ K_{24} = K_{42} = -\frac{AB_{11}}{L}$$

$$K_{34} = K_{43} = 0$$

$$K_{22} = -\frac{1}{10}\frac{AL\{D_{11}L^3 - 10B_{11}\gamma L^2 + 60A_{55}L + 60\eta^2 A_{11}L + 120\gamma B_{11}\eta\}}{(12\eta - L^2)^2}$$

$$K_{23} = K_{32} = \frac{6}{5}\frac{A}{L}\frac{[D_{11}L^4 + 10A_{55}L^2 + 10\gamma^2 L^2 A_{11} - 20L^2 D_{11}\eta + 120D_{11}\eta^2]}{(12\eta - L^2)^2}$$

$$K_{25} = K_{52} = -\frac{6}{5}\frac{A}{L}\frac{[D_{11}L^4 + 10A_{55}L^2 + 10\gamma^2 L^2 A_{11} - 20L^2 D_{11}\eta + 120D_{11}\eta^2]}{(12\eta - L^2)^2}$$

$$K_{26} = K_{62} = \frac{1}{10}\frac{AL[-D_{11}L^3 - 10B_{11}\gamma L^2 - 60A_{55}L - 60\gamma^2 A_{11}L + 120\gamma B_{11}\eta]}{(12\eta - L^2)^2}$$

$$K_{33} = \frac{\{A(2L^6 D_{11} - 30L^4 D_{11}\eta + 180L^2 D_{11}\eta^2 - 15L^5\gamma B_{11} + 2160A_{55}\eta^2 + 60A_{55}L^4 - 360A_{55}\eta L^2 + 180\gamma L^3 B_{11}\eta + 45\gamma^2 L^4 A_{11})\}}{15L(12\eta - L^2)^2}$$

$$K_{35} = K_{53} = \frac{1}{10}\frac{AL\{D_{11}L^3 - 10B_{11}\gamma L^2 + 60A_{55}L + 60\gamma^2 A_{11}L + 120\gamma B_{11}\eta\}}{(12\eta - L^2)^2}$$

$$K_{36} = K_{63} = \frac{-A[L^6 D_{11} - 60A_{55}L^4 - 90\gamma^2 L^4 A_{11} - 60L^4 D_{11}\eta + 360L^2 D_{11}\eta^2 + 4320A_{55}\eta^2 - 720A_{55}\eta L^2]}{30L(12\eta - L^2)^2}$$

$$K_{44} = \frac{AA_{11}}{L}$$

$$K_{45} = K_{54} = \frac{AB_{11}}{L}$$

$$K_{46} = K_{64} = 0$$

$$K_{55} = \frac{6}{5}\frac{A}{L}\frac{\{D_{11}L^4 + 10A_{55}L^2 + 10\gamma^2 L^2 A_{11} - 20L^2 D_{11}\eta + 120D_{11}\eta^2\}}{(12\eta - L^2)^2}$$

$$K_{56} = K_{65} = -\frac{1}{10}\frac{AL\{-D_{11}L^3 - 10B_{11}\gamma L^2 - 60A_{55}L - 60\gamma^2 A_{11}L + 120\gamma B_{11}\eta\}}{(12\eta - L^2)^2}$$

$$K_{66} = \frac{\{A(2L^6 D_{11} + 15L^5\gamma B_{11} - 30L^4 D_{11}\eta + 60A_{55}L^4 + 45\gamma^2 L^4 A_{11} - 180\gamma L^3 B_{11}\eta + 180L^2 D_{11}\eta^2 - 360A_{55}\eta L^2 + 2160A_{55}\eta^2)\}}{15L(12\eta - L^2)^2}$$

The mass matrix for the sandwich beam element is obtained using Eqn. (61) as

$$[M] = \begin{bmatrix} M_{11} & M_{12} & M_{13} & M_{14} & M_{15} & M_{16} \\ M_{21} & M_{22} & M_{23} & M_{24} & M_{25} & M_{26} \\ M_{31} & M_{32} & M_{33} & M_{34} & M_{35} & M_{36} \\ M_{41} & M_{42} & M_{43} & M_{44} & M_{45} & M_{46} \\ M_{51} & M_{52} & M_{53} & M_{54} & M_{55} & M_{56} \\ M_{61} & M_{62} & M_{63} & M_{64} & M_{65} & M_{66} \end{bmatrix},$$

where

$$M_{11} = \frac{1}{3}LI_1, \quad M_{12} = M_{21} = \frac{1}{2}\frac{\gamma L^2 I_1}{(12\eta - L^2)}$$

$$M_{13} = M_{31} = -\frac{1}{4}\frac{\gamma L^3 I_1}{(12\eta - L^2)}$$

$$M_{14} = M_{41} = \frac{1}{6}LI_1$$

$$M_{15} = M_{51} = -\frac{1}{2}\frac{\gamma L^2 I_1}{(12\eta - L^2)}$$

$$M_{16} = M_{61} = -\frac{1}{4}\frac{\gamma L^3 I_1}{(12\eta - L^2)}$$

$$M_{22} = \frac{1}{35}\frac{L[-294I_3\eta L^2 + 35I_2 L^3 + 1680I_3\eta^2 + 13I_3 L^4 - 420I_2\eta L + 42I_1 L^2 + 42\gamma^2 I_1 L^2]}{(12\eta - L^2)^2}$$

$$M_{23} = M_{32} = \frac{\{-L(11I_3 L^5 - 10080I_2\eta^2 + 1260I_3\eta^2 L - 231I_3 L^3\eta + 126\gamma^2 I_1 L^3 + 1260LI_1\eta + 840I_2\eta L^2 + 21I_1 L^3)\}}{210(12\eta - L^2)^2}$$

$$M_{24} = M_{42} = \frac{1}{2}\frac{\gamma L^2 I_1}{(12\eta - L^2)}$$

$$M_{25} = M_{52} = \frac{3}{70}\frac{L[3I_3 L^4 - 28\gamma^2 I_1 L^2 - 28I_1 L^2 - 84I_3\eta L^2 + 560I_3\eta^2]}{(12\eta - L^2)^2}$$

$$M_{26} = M_{62} = \frac{[L(13I_3 L^5 + 10080I_2\eta^2 + 2520I_3\eta^2 L - 378I_3 L^3\eta - 252\gamma^2 I_1 L^3 - 2520LI_1\eta - 840I_2\eta L^2 - 42I_1 L^3)]}{420(12\eta - L^2)^2}$$

$$M_{33} = \frac{[L(252I_3\eta^2 L^2 - 42I_3 L^4\eta + 63\gamma^2 I_1 L^4 - 420I_1\eta L^2 - 2520I_2\eta^2 L + 210I_2\eta L^3 + 10080I_1\eta^2 + 28I_1 L^4 + 2I_1 L^6)]}{210(12\eta - L^2)^2}$$

$$M_{34} = M_{43} = -\frac{1}{4}\frac{\gamma L^3 I_1}{(12\eta - L^2)}$$

$$M_{35} = M_{53} = \frac{[L\,(13 I_3 L^5 - 10080 I_2 \eta^2 + 2520 I_3 \eta^2 L - 378 I_3 L^3 \eta - 252\,\gamma^2 I_1 L^3 - 2520 L I_1 \eta + 840 I_2 \eta L^2 - 42 I_1 L^3)]}{420\left(12\eta - L^2\right)^2}$$

$$M_{36} = M_{63} = \frac{[-L\,(504 I_3 \eta^2 L^2 - 84 I_3 L^4 \eta - 126\gamma^2 I_1 L^4 - 840 I_1 \eta L^2 - 10080 I_1 \eta^2 + 14 I_1 L^4 + 3 I_3 L^6)]}{420\left(12\eta - L^2\right)^2}$$

$$M_{44} = \frac{1}{3} L I_1,\ M_{45} = M_{54} = -\frac{1}{2}\frac{\gamma L^2 I_1}{\left(12\eta - L^2\right)}$$

$$M_{46} = M_{64} = -\frac{1}{4}\frac{\gamma L^3 I_1}{\left(12\eta - L^2\right)}$$

$$M_{55} = \frac{1}{35}\frac{[L(13 I_3 L^4 - 35 I_2 L^3 + 42\gamma^2 I_1 L^2 + 42 I_1 L^2 - 294 I_3 \eta L^2 + 420 I_2 \eta L + 1680 I_3 \eta^2)]}{\left(12\eta - L^2\right)^2}$$

$$M_{56} = M_{65} = \frac{[L\,(11 I_3 L^5 - 231 I_3 L^3 \eta + 126\gamma^2 I_1 L^3 - 840 I_2 \eta L^2 + 21 I_1 L^3 + 1260 L I_1 \eta + 1260 I_3 \eta^2 L + 10080 I_2 \eta^2)]}{210\left(12\eta - L^2\right)^2}$$

$$M_{66} = \frac{[L\,(252 I_3 \eta^2 L^2 - 42 I_3 L^4 \eta + 63\gamma^2 I_1 L^4 - 420 I_1 \eta L^2 + 2520 I_2 \eta^2 L - 210 I_2 \eta L^3 + 10080 I_1 \eta^2 + 28 I_1 L^4 + 2 I_3 L^6)]}{210\left(12\eta - L^2\right)^2}$$

NOMENCLATURE (LIST OF SYMBOLS)

A	Area of the piezo patches
a_1, a_2, a_3, a_4	Polynomial coefficients for transverse displacement
$\mathbf{A}$	System matrix which represents dynamics of system (comprises of mass and stiffness of system)
A_{11}, A_{55}	Extensional and shear stiffness coefficient
B_{11}	Bending-extensional stiffness coefficient
$\mathbf{B}$	Input matrix
b_1, b_2, b_3	Polynomial coefficients for
c	Width of the beam
c_1, c_2, c_3	Polynomial coefficients for axial displacement
$\mathbf{C}$	Output matrix
$\mathbf{C}^*$	Generalized damping matrix or the structural modal damping matrix
$\mathbf{C}_0$	Fictitious matrix
$\mathbf{D}$	Transmission matrix
$\mathbf{D}_0$	Fictitious matrix
D_{11}	Bending stiffness coefficient
D	Layer constitutive matrix
D_3	Electric displacement in the thickness direction
d_{15}, d_{31}	Piezoelectric strain constants
E_{11}	Actuator induced axial force
e_{15}	Piezoelectric constant
E_f	Electric potential applied to the actuator
$\mathbf{E}$	External load matrix, which couples the disturbance to the system
$\mathbf{f}_{ext}$	Vector of externally applied nodal forces
f^t	Total force vector
$\mathbf{f}_{ctrl}$	Control force vector
$\mathbf{f}^*_{ext}, \mathbf{f}^*_{ctrl}$	Generalized external force coefficient and external control force coefficient vector
$\mathbf{f}^*_{ctrl\,1}, \mathbf{f}^*_{ctrl\,2}$	Control force coefficient vectors to the actuators 1 and 2
F_{11}	Actuator induced bending moment
F	State feedback gain
F_1 and F_2	Forces at node 1 and 2 of figure 1
G_{55}	Actuator induced shear force
G_c	Signal conditioning gain
G	Modulus of rigidity
$\mathbf{g}$	Principal coordinates
$\overline{h}$	Height of the beam + the piezo-patches
$\mathbf{h}$	Constant vector, which depends on the type of actuator and its FE position
$\mathbf{h}_1, \mathbf{h}_2$	Constant vectors of the actuators 1 and 2
I_1, I_2, I_3	Mass inertias
I	Inertia matrix
i	Variable (1, 2, 3, …)
$i(t)$	Current induced by the sensor surface
$\mathbf{K}, \mathbf{K}^*$	Stiffness matrix (global stiffness matrix) and generalized stiffness matrix of the beam
k	Variable (1, 2, 3, …)
K_c	Gain of the controller
K	Shear correction factor = 5/6
K_{ij}	Elements of the stiffness matrix $(i, j = 1, 2, ..., 6)$ for the sandwich / composite beam
$\mathbf{L}$	Fast output sampling feedback gain

L	Length of the beam
L_p	Length of the piezo-patch (sensor / actuator)
L_j	Output feedback gains
$\mathbf{M}, \mathbf{M}^*$	Mass matrix (global mass matrix) and generalized mass matrix of the beam
M_{ij}	Elements of the mass matrix $(i, j = 1, 2, ..., 6)$ for the sandwich / composite beam
M_1 and M_2	Moments acting at node 1 and 2 of figure 1
M_x	Internal force on the cross section of the beam
N_u, N_w, N_θ	Shape functions due to axial displacement, transverse displacement and rotation or the slope
$N_1, ..., N_6$	Elements of shape function due to axial displacement
$N_7, ..., N_{10}$	Elements of shape function due to transverse displacement
$N_{11}, ..., N_{14}$	Elements of shape function due to rotation or slope
n	Number of layers of the beam
N	Number of sub-intervals
N	Matrix of shape functions
N_x	Internal force on the cross section of the beam
$\mathbf{p}$	Constant vector, which depends on the sensor type and its FE location in the embedded structure
$\mathbf{p}_1, \mathbf{p}_2$	Constant vectors of the sensors 1 and 2
$q(t)$	Charge accumulated on the sensor surface
$\dot{q}(t)$	Rate of change of electric charge, i.e., the current produced by sensor
$\mathbf{q}$	Vector of nodal displacements (modal coordinate vector), i.e., the generalized coordinates
q_0	Transverse distributed loading
$r(t)$	External force input to the beam
$\dot{\mathbf{q}}$	Time derivative of the nodal coordinate vector
$\ddot{\mathbf{q}}$	Nodal acceleration vector
$Q_{11}, Q_{12}, Q_{13}, Q_{22}, Q_{55}, Q_{66}$	Material constants of steel, foam, PE
Q_{xz}	Internal force on the cross section of the beam
$\mathbf{T}$	Modal matrix containing the eigen values representing the first 3 modes of vibration
t	Time
T	Kinetic energy
t	Total thickness of the beam (top layer + piezo-patch + bottom layer thickness)
t_k	Thickness of the each layer of the beam $k = 1, 2, 3$
t_p	Thickness of the piezoelectric layer
$t_a = t_s = t_p$	Thickness of actuator / sensor = thickness of the piezoelectric layer
u	Axial displacement of the point
u_1, u_2	Axial displacements at fixed end and at free end
$u_1(t), u_2(t)$	Control inputs to actuators 1 and 2
U	Strain energy
$\mathbf{V}^a, \mathbf{V}^s$	Actuator input voltage and sensor voltage

REFERENCES

[1] S.M. Yang, and Y.J. Lee, "Optimization of non-collocated sensor / actuator location and feedback gain in control systems," *Smart materials and Structures*, vol. 8, pp. 157-166, 1993.

[2] E. Crawley, and J. Luis, "Use Of Piezoelectric Actuators As Elements Of Intelligent Structures," *AIAA Journal*, vol.25, no. 10, pp. 1373-1385, 1987.

[3] S. Hanagud, M.W. Obal, and A.J. Callise, "Optimal Vibration Control By The Use Of Piezoelectric Sensors And Actuators," *Journal of Guidance Control and Dynamics,* vol. 15, no. 5, pp. 1199 - 1206, 1992.

[4] B. Bona, M. Indri, and A. Tornamble, "Flexible Piezoelectric Structures-Approximate Motion Equations and Control Algorithms," *IEEE Transactions on Automatic Control*, vol. 42, no. 1, pp. 94- 101, 1997.

[5] J.E. Hubbard Jr., and T. Baily, "Distributed Piezoelectric Polymer Active Vibration Control Of A Cantilever Beam," *Journal Guidance Dynamics and Control*, vol. 8, no. 5, pp. 605 - 611, 1985.

[6] S. Rao, and M. Sunar, "Piezoelectricity And Its Uses In Disturbance Sensing And Control of Flexible Structures: A Survey," *Applied Mechanics Rev.*, vol. 47, no. 2, pp. 113 - 119, 1994.

[7] Yong-Yan Cao, J. Lam, and Y.X. Sun, "Static Output Feedback Stabilization: An LMI Approach", *Automatica*, vol. 34, no. 12, pp. 1641-1645, 1998.

[8] P. Donthireddy, and K. Chandrashekhara, "Modeling and Shape Control of Composite Beam with Embedded Piezoelectric Actuators", *Composite Structures*, vol. 35, no. 2, pp. 237- 244, 1996.

[9] C.T. Sun, and X.D. Zhang, "Use of Thickness-Shear Mode in Adaptive Sandwich Structures", *Smart Materials and Structures*, vol. 4, no. 3, pp. 202 - 206, 1995.

[10] W. Hwang, and H.C. Park, "Finite Element Modeling of Piezoelectric Sensors and Actuators", *AIAA Journal*, vol. 31, no. 5, pp. 930-937, 1993.

[11] C. Doschner, and M. Enzmann, "On Model based Controller Design for Smart Structure", *Smart Mechanical Systems Adaptronics SAE International USA*, pp. 157-166, , 1998.

[12] K. Chandrashekhara, and S. Varadarajan, "Adaptive Shape Control of Composite Beams with Piezoelectric Actuators", *J. of Intelligent Materials Systems and Structures,* vol. 8, pp. 112-124, 1997.

[13] O.J. Aldraihem, R.C. Wetherhold, and T. Singh, "Distributed Control of Laminated Beams: Timoshenko vs. Euler-Bernoulli Theory", *Journal of Intelligent Materials Systems and Structures*, vol. 8, pp. 149-157, 1997.

[14] H. Abramovich, "Deflection Control of Laminated Composite Beam with Piezoceramic Layers-Closed Form Solution", *Composite Structures*, vol. 43, no. 3, pp. 217-231, 1998.

[15] X.D. Zhang, and C.T. Sun, "Formulation of an Adaptive Sandwich Beam", *Smart Materials and Structures*, vol. 5, no. 6, pp. 814–823, 1996.

[16] S. Raja, G. Prathap, and P.K. Sinha, "Active Vibration Control of Composite Sandwich Beams with Piezoelectric Extension-Bending and Shear Actuators", *Smart Materials and Structures*, vol. 11, no. 1, pp. 63-71, 2002,
[17] A. Benjeddou, M.A. Trindade, and R. Ohayon, "New Shear Actuated Smart Structure Beam Finite Element", *AIAA Journal*, vol. 37, pp. 378 - 383, 1998.
[18] O.J. Aldraihem, and A.A. Khdeir, "Smart Beams with Extension and Thickness-Shear Piezoelectric Actuators", *Smart Materials and Structures*, vol. 9, no. 1, pp. 1- 9, 2000.
[19] V.L. Syrmos, P. Abdallah, P. Dorato, and K. Grigoriadis, "Static Output Feedback A Survey", *Automatica*, vol. 33, no. 2, pp. 125-137, 1997.
[20] H. Werner, and K. Furuta, "Simultaneous Stabilization Based on Output Measurements", *Kybernetika*, vol. 31, no. 4, pp. 395 - 411, 1995
[21] Herbert Werner, 1998, "Multimodal Robust Control by Fast Output Sampling-An LMI Approach," *Automatica*, Vol. 34, No. 12, pp. 1625-1630.
[22] B. Culshaw, "Smart Structure A Concept or A Reality," *Journal of Systems and Control Engg.*, vol. 26, no. 206, pp. 1-8, 1992.
[23] T. C. Manjunath, and B. Bandyopadhyay, "Vibration control of a smart flexible cantilever beam using periodic output feedback," *Asian Journal of Control*, vol. 6, no. 1, pp. 74 - 87, Mar. 2004.
[24] T. C. Manjunath, and B. Bandyopadhyay, "Fault tolerant control of flexible smart structures using robust decentralized periodic output sampling feedback technique," *International Journal of Smart Materi. and Struct.*, vol. 14, no. 4, pp. 624-636, Aug. 2005.
[25] T. C. Manjunath, and B. Bandyopadhyay, "Control of vibrations in flexible smart structures using FOS feedback technique," *Int. Journal of Computational Intelligence*, vol. 3, no. 2, pp. 127-141, Apr. 2006.
[26] J. B. Kosmataka, and Z. Friedman, "An improved two-node Timoshenko beam finite element", *Computers and Struct.*, vol. 47, no. 3, pp. 473 - 481, 1993.
[27] L. E. Azulay, and H. Abramovich, "Piezoelectric actuation and sensing mechanisms-Closed form solutions," *Composite Structures J.*, vol. 64, pp. 443 - 453, 2004.
[28] A. K. Ahmed, and J. A. Osama, "Deflection analysis of beams with extension and shear piezoelectric patches using discontinuity functions" *Smart Materials and Structures*, vol. 10, no. 1, pp. 212 - 220, 2001.
[29] J.S.M. Moita, I.F.P. Coreia, C.M.M. Soares, and C.A.M. Soares, "Active Control of Adaptive Laminated Structures With Bonded Piezoelectric Sensors and Actuators," in *Computers and Structures*, 82, 1349 - 1358, 2004.
[30] J.A. Zapfe, and G.A. Lesieutre, "A Discrete Layer Beam Finite Element for The Dynamic Analysis of Composite Sandwiched Beams With Integral Damping Layers," in *Computers and Structures*, vol. 70, pp. 647 - 666, 1999.
[31] J. Lee, "Free Vibration Analysis of Delaminated Composite Beams," in *Computers and Structures*, vol. 74, pp. 121 - 129, 2000.
[32] R.C. Louis, C.S. Edward, and M. Brian, "Induced Shear Piezoelectric Actuators for Rotor Blade Trailing Edge Flaps," in *Smart Materials and Structures*, vol. 11, pp. 24 - 35, 2002.
[33] H. Abramovich, and A. Lishvits, "Free Vibrations of Non-symmetric Cross-ply Laminated Composite Beams," in *Journal of Sound and Vibration*, vol. 176, no. 5, pp. 597 - 612, 1994.
[34] J.L. Fanson, and *et al.*, "Positive position feedback control for structures," *AIAA J.*, vol. 18, no. 4, pp. 717 - 723, 1992.
[35] P. Seshu, "Textbook of Finite Element Analysis," 1st Ed. Prentice Hall of India, New Delhi, 2004.
[36] M. Umapathy, and B. Bandyopadhyay, "Control of flexible beam through smart structure concept using periodic output feedback," *System Science Journal*, vol. 26, no. 1, pp. 23 - 46, 2000.
[37] T. C. Manjunath, and B. Bandyopadhyay, "Modeling and fast output sampling feedback control of a smart Timoshenko cantilever beam", Smart Structures and Systems, vol. 1, no. 3, pp. 283–308, Sept. 2005.

T. C. Manjunath, born in Bangalore, Karnataka, India on Feb. 6, 1967 received the B.E. Degree in Electrical Engineering from the University of Bangalore in 1989 in First Class and M.E. in Automation and Control Engineering with specialization in Automation, Control and Robotics from the University of Gujarat in 1995 in First Class with Distinction, respectively. He has got a teaching experience of 17 long years in various engineering colleges all over the country and is currently working as a Research Engineer in the department of systems and control engineering, Indian Institute of Technology Bombay, India and simultaneously doing his Ph.D. in the Interdisciplinary Programme in Systems and Control Engineering, Indian Institute of Technology Bombay, Powai, Mumbai-400076, India, in the field of modeling, simulation, control and implementation of smart flexible structures using DSpace and its applications. He has published 64 papers in the various national, international journals and conferences and published two textbooks on Robotics, one of which has gone upto the third edition and the other, which has gone upto the fourth edition along with the CD which contains 200 C / C++ programs for simulations on robotics. He is a student member of IEEE since 2002, SPIE student member and IOP student member since 2004, life member of ISSS and a life member of the ISTE, India. His biography was published in 23rd edition of Marquis' Who's Who in the World in 2006 issue. He has also guided more than 2 dozen robotic projects. His current research interests are in the area of Robotics, Smart Structures, Control systems, Network theory, Mechatronics, Process Control and Instrumentation, CT and DT signals and systems, Signal processing, Periodic output feedback control, Fast output feedback control, Sliding mode control of SISO and multivariable systems and its applications.

B. Bandyopadhyay, born in Birbhum village, West Bengal, India, on 23rd August 1956 received his Bachelor's degree in Electronics and Communication Engineering from the University of Calcutta, Calcutta, India, and Ph.D. in Electrical Engineering from the Indian Institute of Technology, Delhi, India in 1978 and 1986, respectively. In 1987, he joined the Interdisciplinary Programme in Systems and Control Engineering, Indian Institute of Technology Bombay, India, as a faculty member, where he is currently a Professor. He visited the Center for System Engineering and Applied Mechanics, Universite Catholique de Louvain, Louvain-la-Neuve, Belgium, in 1993. In 1996, he was with the Lehrstuhl fur Elecktrische Steuerung und Regelung, Ruhr Universitat Bochum, Bochum, Germany, as an Alexander von Humboldt Fellow. He revisited the Control Engineering Laboratory of Ruhr University of Bochum during May-July 2000. He has authored and coauthored 7 books and book chapters, 52 national and international journal papers and 123 conference papers, totaling to 182 publications. His research interests include the areas of large-scale systems, model reduction, reactor control, smart structures, periodic output feedback control, fast output feedback control and sliding mode control. Prof. Bandyopadhyay served as Co-Chairman of the International Organization Committee and as Chairman of the Local Arrangements Committee for the IEEE International Conference in Industrial Technology, held in Goa, India, in Jan. 2000. His biography was published in Marquis' Who's Who in the World in 1997. Prof. B. Bandyopadhyay has been nominated as one of the General Chairmen of IEEE ICIT conference to be held in Mumbai, India in December 2006 and sponsored by the IEEE Industrial Electronics Society.